





Review

Recent Advances in BODIPY Compounds: Synthetic Methods, Optical and Nonlinear Optical Properties, and Their Medical Applications

Prabhuodeyara M. Gurubasavaraj ^{1,*}, Vinodkumar P. Sajjan ¹, Blanca M. Muñoz-Flores ²,
Víctor M. Jiménez Pérez ^{2,*} and Narayan S. Hosmane ^{3,*}

¹ Department of Chemistry, Rani Channamma University, Belagavi 591156, India; vinodkumarsjjn@gmail.com

² Facultad de Ciencias Químicas, Universidad Autónoma de Nuevo León, San Nicolás de los Garza 66451, Nuevo León, Mexico; blanca.munozfl@uanl.edu.mx

³ Department of Chemistry and Biochemistry, Northern Illinois University, DeKalb, IL 60115, USA

* Correspondence: pmg@rcub.ac.in (P.M.G.); victorjimenezpr@uanl.edu.mx (V.M.J.P.); hosmane@niu.edu (N.S.H.)

Abstract: Organoboron compounds are attracting immense research interest due to their wide range of applications. Particularly, low-coordinate organoboron complexes are receiving more attention due to their improbable optical and nonlinear optical properties, which makes them better candidates for medical applications. In this review, we summarize the various synthetic methods including multicomponent reactions, microwave-assisted and traditional pathways of organoboron complexes, and their optical and nonlinear properties. This review also includes the usage of organoboron complexes in various fields including biomedical applications.



Citation: Gurubasavaraj, P.M.; Sajjan, V.P.; Muñoz-Flores, B.M.; Jiménez Pérez, V.M.; Hosmane, N.S. Recent Advances in BODIPY Compounds: Synthetic Methods, Optical and Nonlinear Optical Properties, and Their Medical Applications. *Molecules* **2022**, *27*, 1877. <https://doi.org/10.3390/molecules27061877>

Academic Editor: Vito Capriati

Received: 16 February 2022

Accepted: 9 March 2022

Published: 14 March 2022

Publisher's Note: MDPI stays neutral with regard to jurisdictional claims in published maps and institutional affiliations.



Copyright: © 2022 by the authors. Licensee MDPI, Basel, Switzerland. This article is an open access article distributed under the terms and conditions of the Creative Commons Attribution (CC BY) license (<https://creativecommons.org/licenses/by/4.0/>).

Keywords: organoboron; synthesis fluorescence; nonlinear optical; imaging

1. N-B-N Environment in Organoboron Compounds

The chemistry of organoboron compounds is one of the most multifaceted research areas among heteroatom-substituted organic molecules. These organoboron compounds have vast applications in numerous fields including biomedical and nuclear chemistry [1–4]. There is a dramatic rise in the research on the applications of boronic acid and their derivatives [5–9]. Boron is an interesting molecule with an electron-deficient character and is also more electropositive than carbon. This rudimentary property of boron has been completely utilized in synthesizing various organoboron compounds and exploring their applications in organic synthesis [10–15].

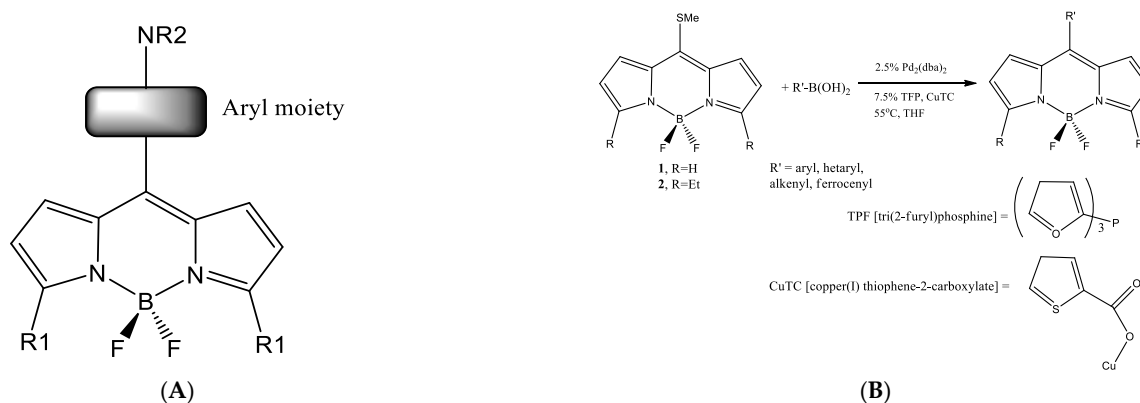
The report by Treibs and Kreuzer on BODIPY derivatives have opened up an exciting and useful field in chemistry. Since then, BODIPY chemistry has grown immensely and reports have poured in for the different ways of synthesis of BODIPY compounds and their applications. These applications include their uses in laser dyes, protein tags, and metal sensors. Fluorescent compounds have seen the limelight as these are most importantly studied by various research communities in multidisciplinary areas. Among all the other fluorescent compounds, boron-containing compounds are of utmost interest these days as they have significant and thrilling applications in various fields as active media of tunable lasers; development of photoelectronic devices, fluorescent probes, and chemical sensors; or monitoring the physicochemical characteristics of the surrounding ambiances. They also have optical features, as these compounds show better photo-stability, robust fluorescence intensity, high quantum yields, and small Stokes shift [16]. Even though these systems are known for intrinsic potential applications, their photophysical properties are highly focused so as to design new dyes with specific properties. This can be performed by changing the molecular structure of the chromophore (substituent effect) and the environmental conditions (solvent effect, incorporation in rigid solid materials, etc.) [17].

In this review, we summarize the various synthetic methods including multicomponent reactions, microwave-assisted and traditional pathways of organoboron complexes, and their optical and nonlinear properties. This review also includes the usage of organoboron complexes in various fields including biomedical applications.

2. Organoboron Compounds Having NBN Framework

In recent times, there has been increasingly immense research interest in BODIPY (boron-dipyrromethene) compounds containing distinct substituent groups (with heteroelements in meso and other positions) based on NBN ligand core [18]. This is due to their attractive properties as they are tunable for fluorescence emission in 500–700 nm regions with high fluorescent quantum yield in various solutions and good photostability [19–22]. These fluorescent compounds have found profound applications as tracers in fluorescence microscopy in fluorescence immunoassay and in flow cytometric analysis, along with a series of other useful applications [23–28].

In this review, we summarize a series of new meso-polyarylamine-BODIPY hybrids of the general structure (A) Scheme 1, which were synthesized by two different modified methods.

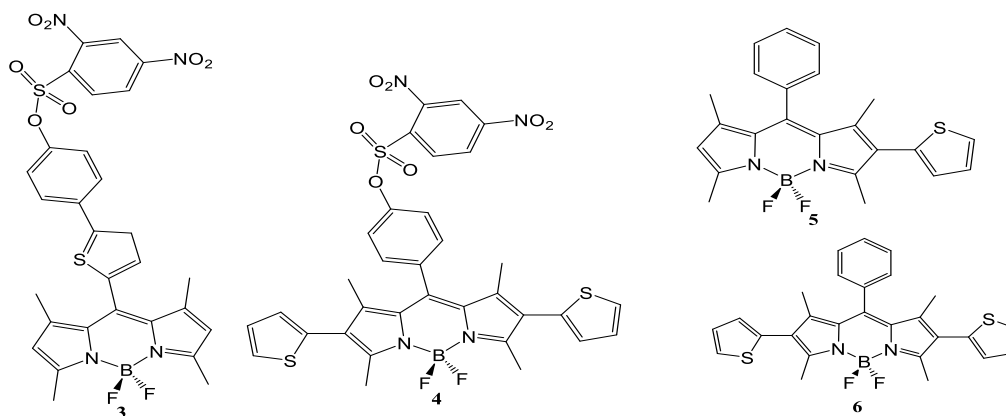


Scheme 1. General synthesis of 8-substituted BODIPYs with the Liebeskind–Srogl cross-coupling.

- (A) Liebeskind–Srogl coupling: Cross-coupling of thiomethyl BODIPYs with arylaminoboronic acids [29].
- (B) Liebeskind–Srogl and Suzuki coupling: By a two-step sequence, a reaction to prepare meso-bromoaryl BODIPYs followed by coupling of these Bromine-containing BODIPYs with arylaminoboronic acids [30–35].

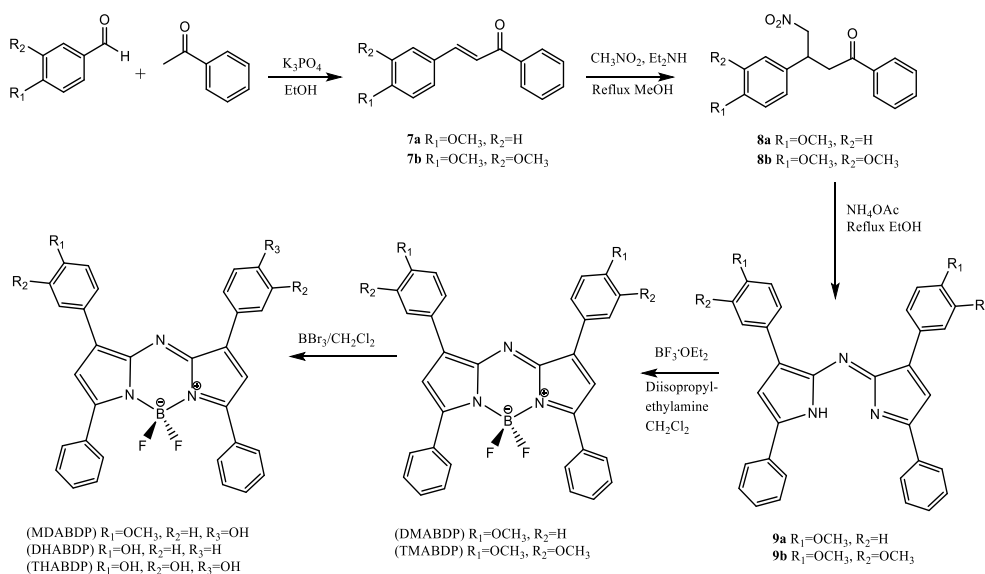
Several of these derivatives exhibited emission in the near-infrared region. BODIPY derivatives of 2-thienyl and 2,6-bisthienyl displayed intense absorption and a large Stokes shift in contrast with the typical BODIPY.

Based on DFT calculations [36–38], it was proposed that the large Stokes shifts of **3**, **4**, and **5** (Scheme 2) are due to the remarkable geometry relaxation upon photoexcitation and its substantial effect on the energy levels of molecular orbitals. For the dyes with small Stokes shifts, much smaller geometry relaxations were found [39–41].



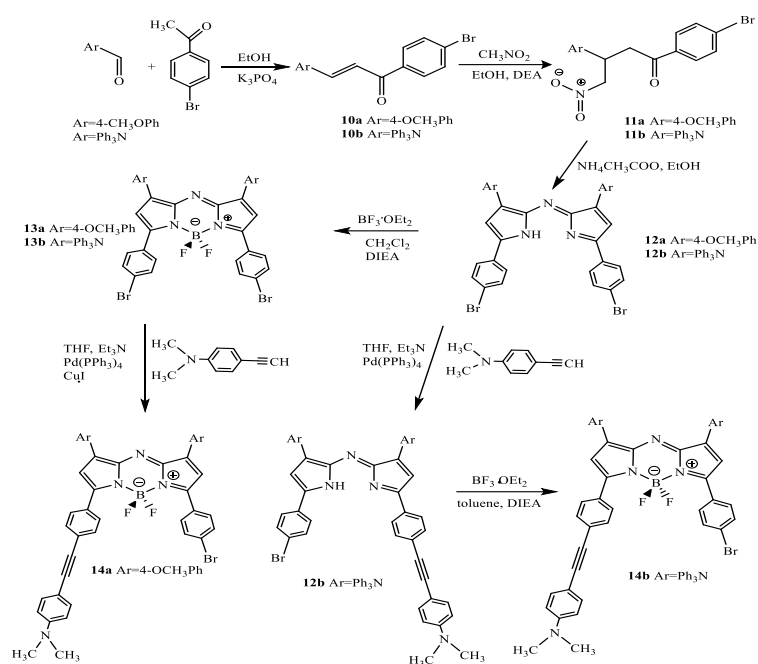
Scheme 2. Compounds **3**, **4**, **5**, and **6** can also be synthesized by the Liebeskind–Srogl and Suzuki coupling.

Several research groups reported [42] the detailed synthesis and reactions of aza-boron-dipyrromethene (Aza-BODIPY) compounds (Scheme 3) containing methoxy and hydroxyl groups. The study on linear absorption spectra for phenolate forms of aza-BODIPY containing hydroxyl group exhibited drastic changes and showed new bands for phenolate groups in the region below 500 nm and above 700 nm in THF solutions. In addition, no fluorescence signals were observed with 600 nm excitation for phenolate forms. Moreover, these hydroxyl group (HABDP)-containing aza-BODIPY compounds revealed two photon absorption properties at 1200–1450 nm spectral range [43].



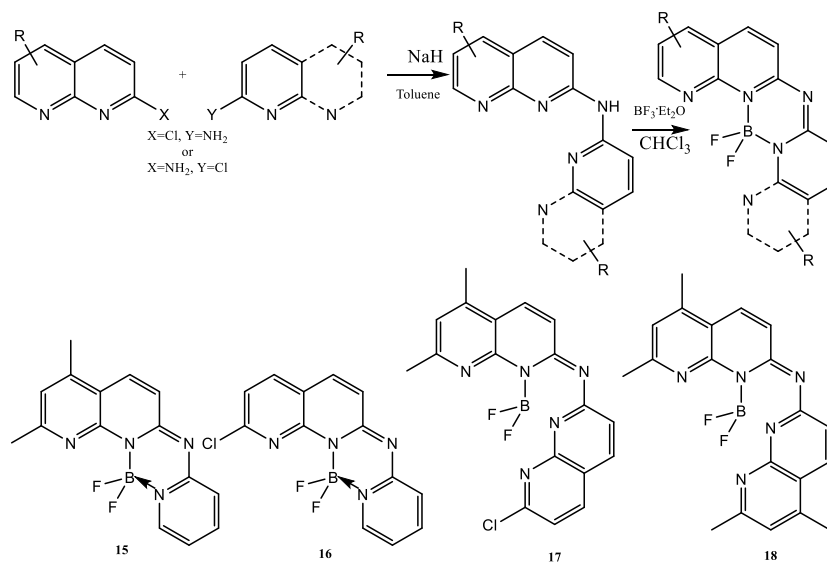
Scheme 3. Structures of methoxy (MABDP) and hydroxy (HABDP) substituted aza-BODIPY.

Reports [44] on the properties of aza-BODIPY containing triphenylamine, 4-ethynyl-N,N-dimethylaniline, and methoxy moieties (Scheme 4) such as substitution and charge transfer on linear and nonlinear optical absorption (especially two-photon absorption) were investigated by ultrafast pump–probe spectroscopy technique. It was observed that aza-BODIPY compounds with good electron-donating moieties (triphenylamine and 4-ethynyl-N,N-dimethylaniline moieties) have charge transfer from electron-donating parts of the molecules to aza-BODIPY core. The two-photon absorption cross sections increase with the electron-donating strength.



Scheme 4. Structures of investigated compounds.

Additionally, 1,8-naphthyridine– BF_2 complexes **15–18** were synthesized (Scheme 5); these are known for their good fluorescence properties. These complexes contain one N atom less between naphthyridine moieties that have strong emissions in the solid state (Figure 1) [45]. Both naphthyridine and pyridine ar units in their structure are ligated to the BF_2 core as monodentate ligands, and the two aromatic units are nearly coplanar with dihedral angles of 4.91 and 2.968 for the B- and N-form crystals, respectively. SEM and TEM images of **17** showed that it consists of tangled nanowires of width about 30 nm and lengths varying from several hundred nanometers to several micrometers (Figure 2).



Scheme 5. Synthetic routes to and chemical structures of 1,8-naphthyridine derivatives **15–18**.

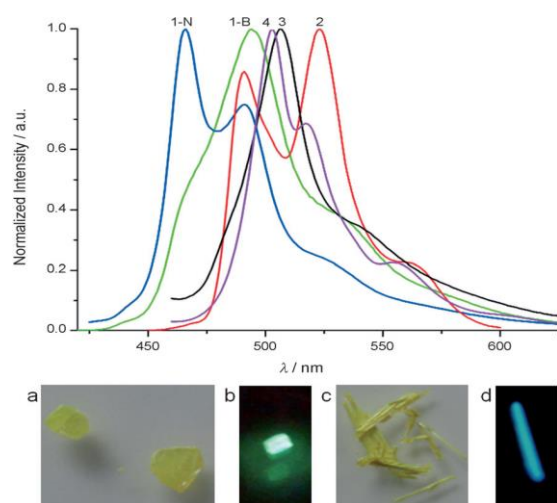


Figure 1. Top: solid-state emissions of complexes 15–18 at room temperature. Bottom: photographs of B-form and N-form crystals of 1 under natural light (a,c) and under 365 nm UV lamp (b,d).

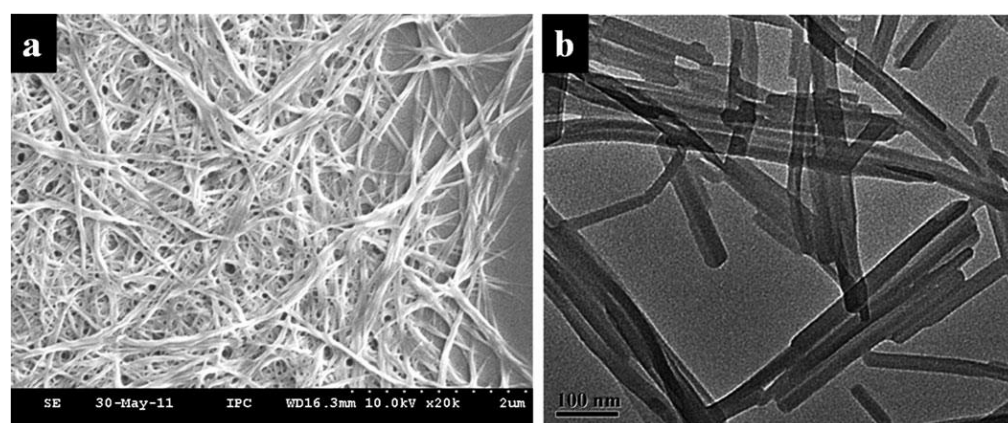


Figure 2. (a) SEM and (b) TEM images of nanowires of 17.

Further, some research groups reported a new dye, BF₂-rigidified anilido-pyridine boron difluoride (Figure 3), which show large Stokes shifts and high photostability [46]. These are air- as well as moisture-stable and do not undergo photodegradation even upon exposure to continuous radiation. This photostability makes the dye more efficient when compared with BODIPY and many other dyes. Their efficacy as probes for biological membranes was demonstrated using a liposome model.

Besides, other aryl and hetaryl moieties in BODIPY compounds are widely reported. Three two-photon active boradiazaindacene derivatives 2,6-di-phenylacetylenyl-1,3,5,7-tetramethyl-8-phenyl-4,4-difluoroboradiazaindacene (Figure 4, 24a), 2,6-di-9-ethyl-9H-carbazole-3-ethynyl-1,3,5,7-tetramethyl-8-phenyl-4,4-difluoroboradiazaindacene (Figure 4, 24b) and 2,6-di-4-N,N-diphenyl-phenylacetylenyl-1,3,5,7-tetramethyl-8-phenyl-4,4-difluoroboradiazaindacene (Figure 4, 24c) in THF solutions were studied by using femto-second laser spectroscopic techniques [47]. The two-photon fluorescence imaging experiment on these compounds exhibit good cell permeability, nontoxicity, and excellent two-photon fluorescence properties. Structurally rigid BODIPY having spirofluorene moieties [48] (Figure 5) were reported that exhibit intense bathochromic fluorescence. These rigid structures give high quantum yield of photoluminescence and decreased nonradiative decay of excited states. DFT calculations indicated that spiro-conjugation leads to delocalization of the π -system of BODIPY derivatives over the fluorene moieties as well as the BODIPY core. Moreover, symmetric BODIPY dyads (Figure 6) have chromophores at the meso

position through phenylene bridge or direct linkage [49]. In excited state, these molecules will undergo symmetry-breaking through ICT state. Due to differences in degree of rotational freedom, these dyads will show different behavior of the ICT state. Whereas dyad **25** undergoes rapid nonradiative decay to the ground state, the more hindered dyad **26** has a long-lived ICT state with moderate-to-high fluorescence quantum efficiency. The excited state properties of these dyads could prove useful in facilitating charge separation in photovoltaic devices.

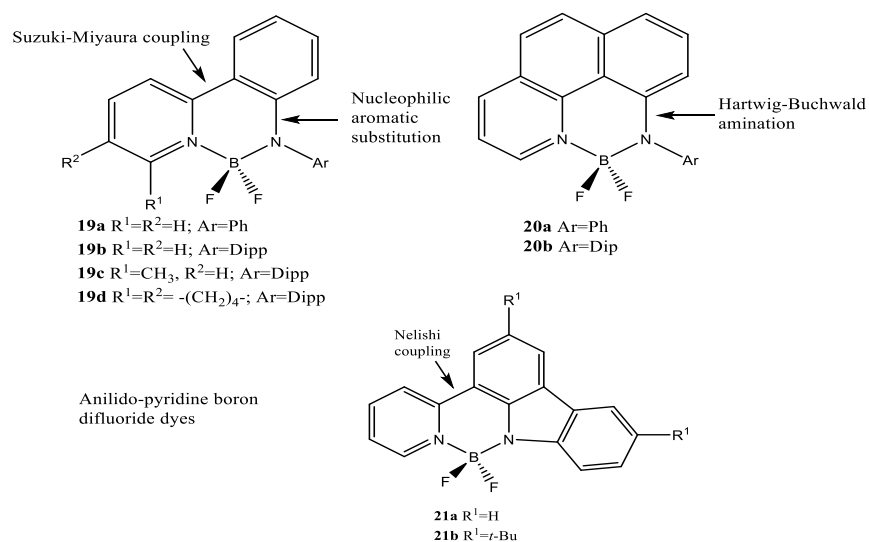


Figure 3. BF_2 -rigidified anilido-pyridine boron difluoride dye.

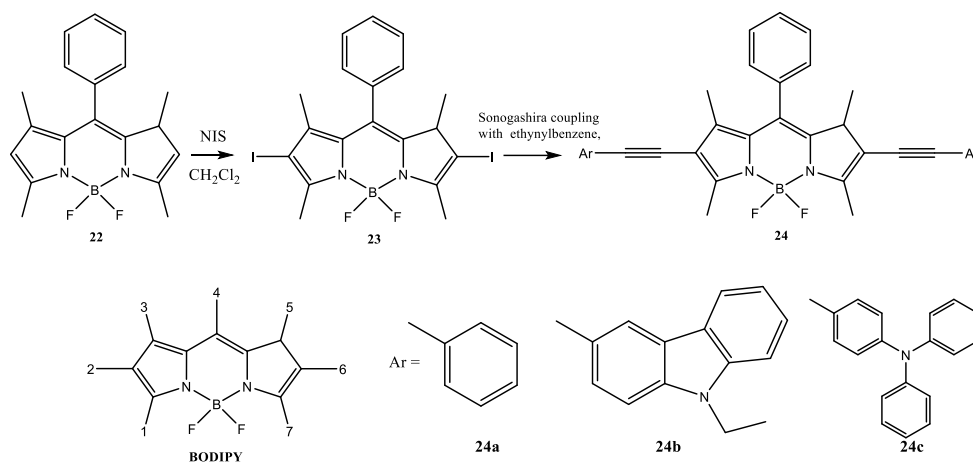


Figure 4. Boradiazaindacene derivatives of **24a**, **24b**, **24c**.

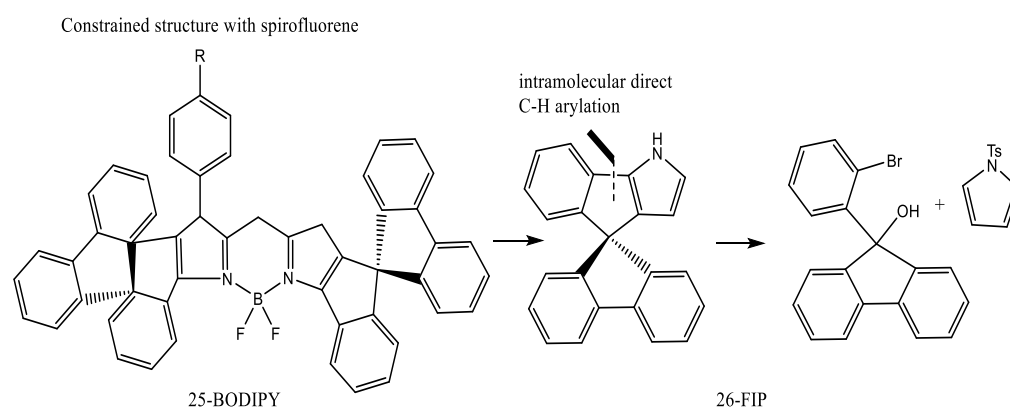


Figure 5. New approach to structurally constrained BODIPY dyes.

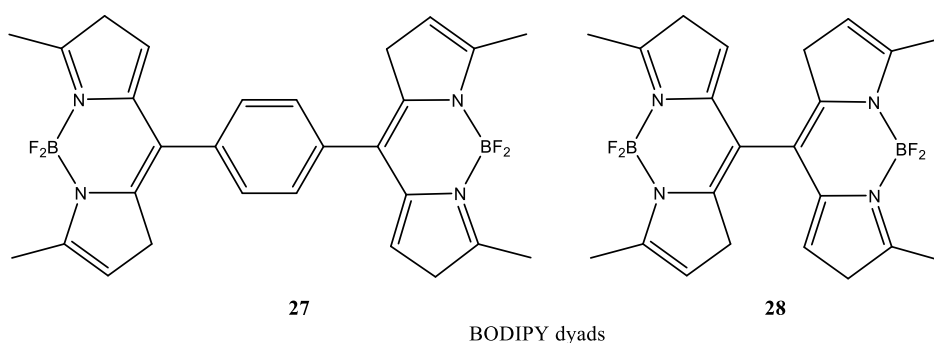


Figure 6. Symmetric BODIPY dyads with chromophores at the meso position.

Introduction of radiotracers in BODIPY compounds is also known [50]. The rapid nucleophilic [^{18}F]-radiolabeling of a BODIPY dye in aqueous solutions is reported (Figure 7). This radiolabeled dye was found to be stable *in vivo* and used as a dual modality imaging agent. Besides several applications of BODIPY compounds, we elucidate that the BODIPY-based fluorescent probe **31** can be used for the selective detection (Figure 8) of tyrosinase (a copper-containing enzyme catalyzing the hydroxylation of phenol derivatives, such as tyrosine or tyramine, which is widespread in plants and animal tissues) activity in buffered aqueous solution [51], is suitable for screening potential inhibitors of tyrosinase, as well as for bioimaging intracellular tyrosinase activity in living cells.

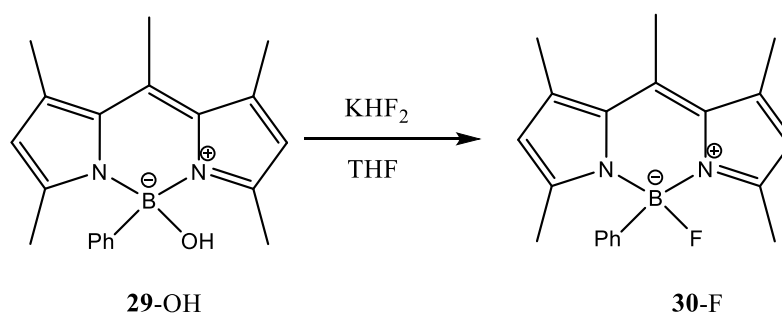


Figure 7. Nucleophilic [^{18}F]-radiolabeling of a BODIPY dye.

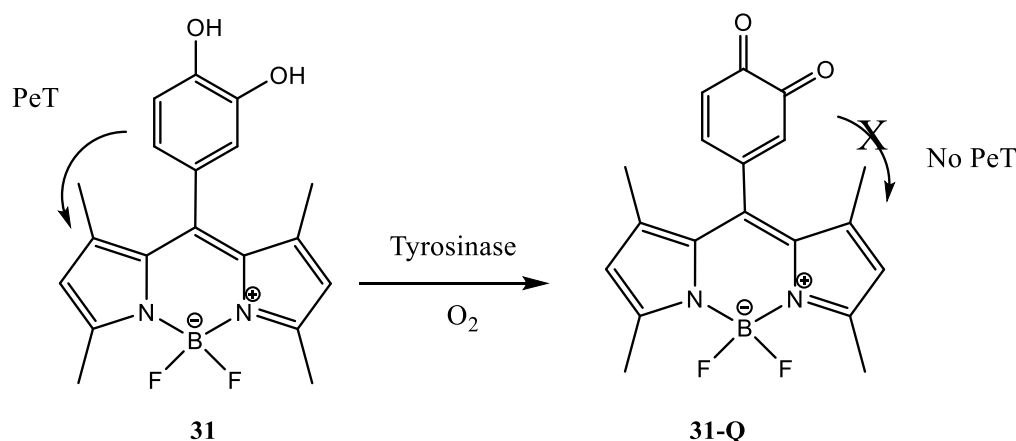
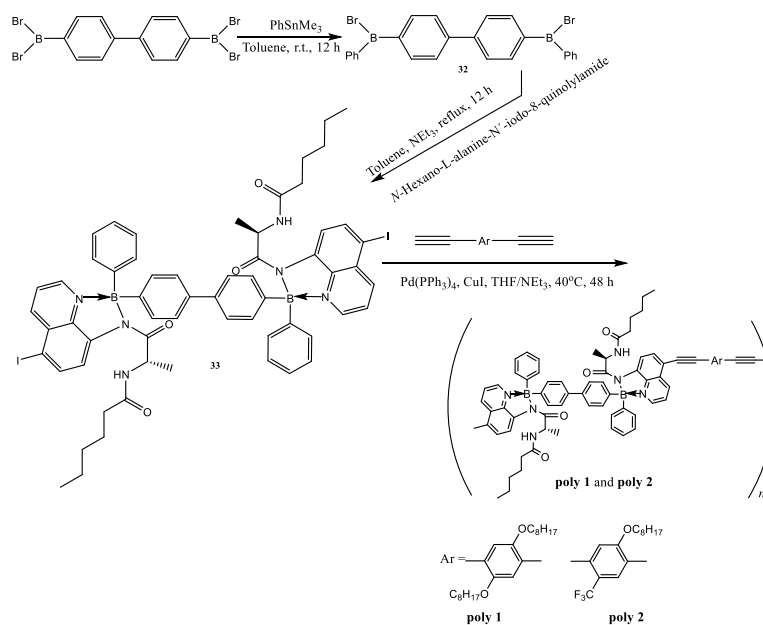


Figure 8. Proposed fluorescence turn-on assay for tyrosinase by probe 31.

Some NBN-environment-based organoboron compounds have also been reported with a wide variety of applications. Thus, optically active organoboron aminoquinolate-based coordination polymers bearing the chiral side chain derived from L-alanine were synthesized (Scheme 6) and their optical behavior was studied by UV–Vis and photoluminescence spectroscopies [52]. The hydrogen-bonding in these polymers was found to be stable in solvents such as CHCl_3 and DMF studies of circular dichroism (CD). Intramolecular charge transfer was observed due to the fact of solvents polarity. Further, some toxic compounds such as Triphenyl borane were studied (Figure 9). The toxicity of the alternative organotin (Ot) antifoulants TPBP (triphenylborane pyridine; Figure 9: 34) and TPBOA (triphenylborane octadecylamine; Figure 9: 35) and their degradation products on *Crassostea gigas* and *Hemicentrotus pulcherrimus* were tested [53]. Silylated-diborylene-3,4,9,10-tetraaminoperylene (DIBOTAPs, compounds 39–42) were synthesized by treating 4,9-diaminoperylenequinone-3,10-diimine (DPDI, Scheme 7) with $\text{BH}_3\text{-THF}$, lithiation with *n*-butyllithium, and subsequent addition of the corresponding silyl chloride (Scheme 8) [54]. In all cases, the perylene backbones were found to be not completely planar. The coordination of the nitrogen donor atoms to the Lewis acidic boron atoms stabilizes the tetraaminoperylene core, while the *N*-silylation appears to suppress aggregation in solution. The latter enables the high luminescence quantum yields. The exchange of all three methyl groups with ethyl (compound 39) or isopropyl (compound 40) substituents resulted in a significant increase in quantum yields with values of 92% and 89%, respectively. The observed fluorescence decay is monoexponential for all dyes with typical lifetimes of 5.5–6.6 ns.

To conclude, 1D boron containing two-photon absorbing fluorophores with two boron-containing central cores (with two boron atoms)—the cyclodiborazane and the pyrazabole moieties—were reported (Scheme 9) [55]. All compounds present a strong two-photon induced fluorescence and have been used in microscopy to visualize cancerous HeLa cells. High boron content should be of great interest to study the mechanism of boron neutron capture therapy by deep imaging in small animals with micrometric resolution by two-photon excited fluorescence.



Scheme 6. Synthesis of organoboron aminoquinolate-based coordination polymers.

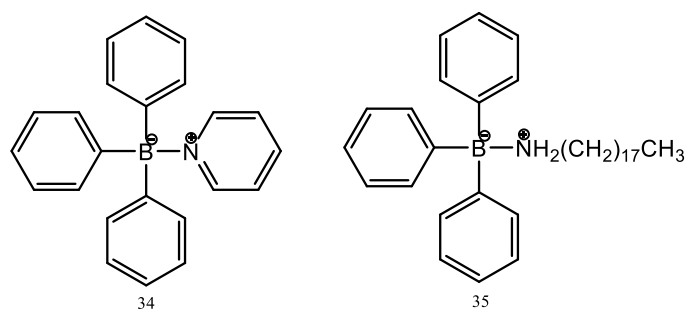
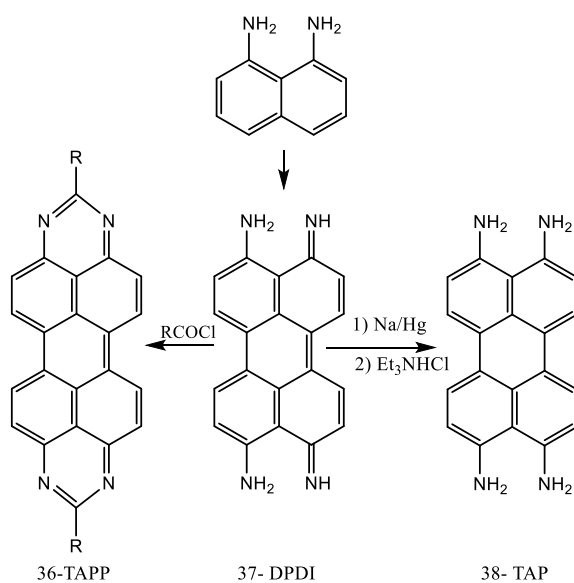
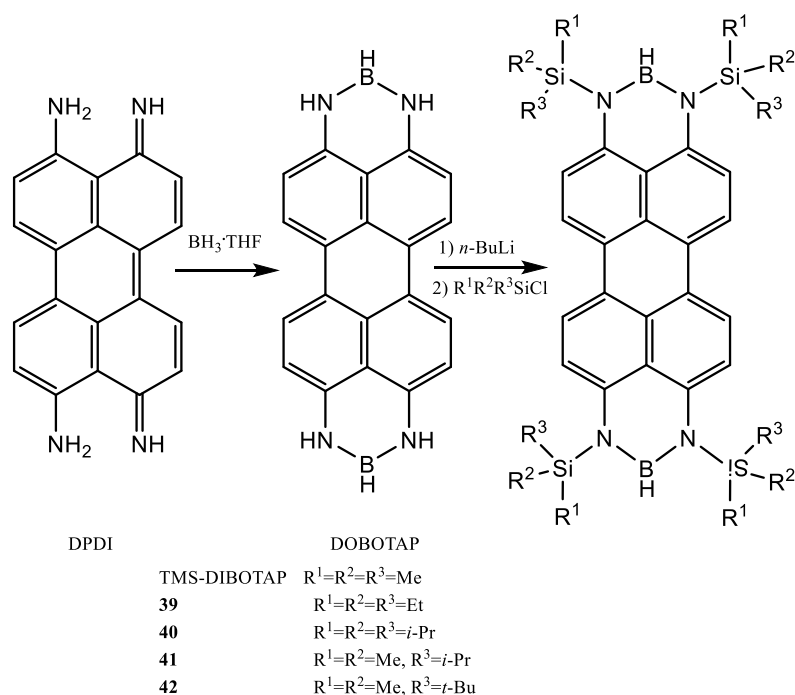


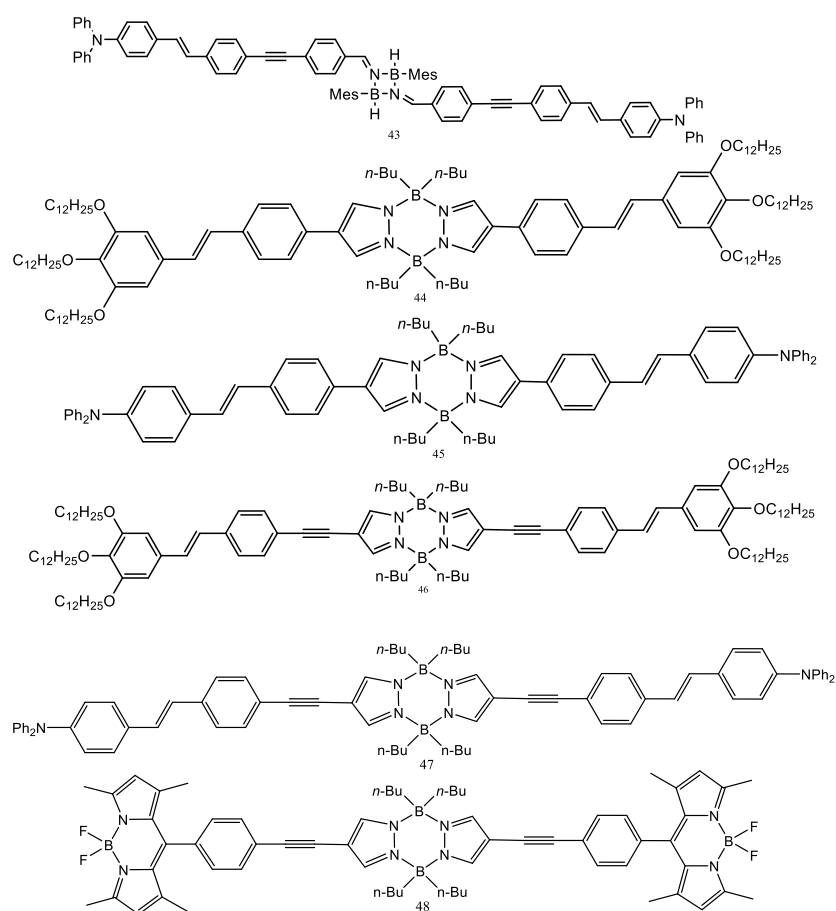
Figure 9. TPBP (34) (triphenylboranepyridine) and TPBOA (35) (triphenylboraneoctadecyl).



Scheme 7. Synthesis of 4,9-diaminoperylenequinone-3,10-diimine (DPDI), 1,3,8,10-tetraazaperylene (TAPP), and 3,4,9,10-tetraaminoperylene (TAP).



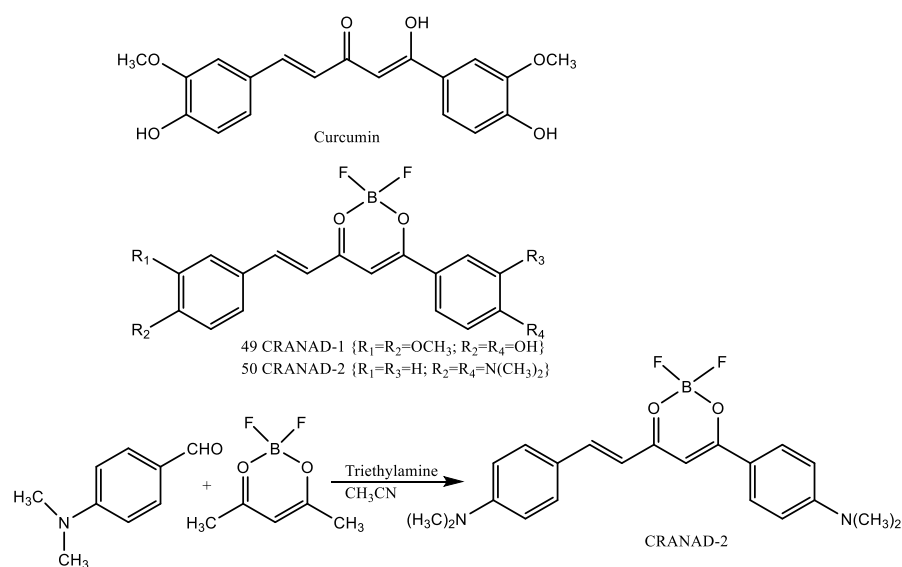
Scheme 8. Synthesis of silylated-diborylene-3,4,9,10-tetraaminoperylene compounds **39–42** and TMS-DIBOTAP.



Scheme 9. Chemical structures of prepared fluorophores based on cyclodiborazane and pyrazabole central cores.

3. Compounds Containing O-B-O Framework

A predominant number of boron compounds containing O-B-O moiety corresponds to β -diketone derivatives, having been extensively studied for their fluorescent properties [56]. Reports on the first difluoroborate diketone compounds that are curcumin-derivatized by the NIR fluorescent probe, CRANAD-2 (Scheme 10), for in vivo biological studies and provides a useful type of NIR fluorescent dye for cell, tissue, and in vivo imaging for small animals [57]. Upon interacting with aggregates, CRANAD-2 undergoes a range of changes, which include a 70-fold fluorescence intensity increase, a 90-nm blue shift (from 805 to 715 nm), and a large increase in quantum yield. After intravenous injection of this probe, 19-month-old Tg2576 mice exhibited significantly higher relative signal than that of the control mice over the same period of time (Figure 10) [58].



Scheme 10. (Top) Structure of curcumin, compound 49 (CRANAD-1), and compound 50 (CRANAD-2); (bottom) synthetic route for CRANAD-2.

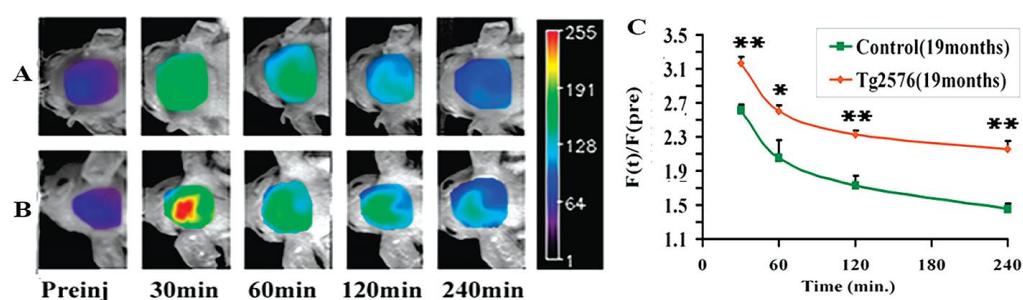


Figure 10. Representative images of Tg2576 mice and control littermates at different time points before and after intravenous injection of 5.0 mg/kg CRANAD-2. (A) 19-month-old control mouse; (B) 19-month-old Tg2576 mouse (mice showed similar background fluorescence signal); (C) the relative fluorescence signal $[F(t)/F(\text{pre})]$ was significantly higher than that of the control mice, and the decay of fluorescence signal was significantly slower in transgenic mice compared with the control group (*: $p < 0.005$, **: $p < 0.01$).

Surprising process-dependent and reversible mechanochromic fluorescence was discovered for the boron dodecane complex (BF₂dbmOC₁₂H₂₅) (Figure 11)—a difluoroboron dibenzoylmethane dye coupled to a lipid chain [59]. A thermally annealed spin-cast film of the lipid dye on glass exhibited blue fluorescence under UV light; however, after shearing or scratching, the mechanically perturbed region turned yellow–green. The blue coloration

could be rapidly recovered by thermal treatment of the film [60]. In order to test the effects of alkyl chain length on solid-state photoluminescence and reversible mechanochromic luminescence (ML) in difluoroboron β -diketonate dyes, a series of dyes, BF_2dbmOR , with dibenzoylmethane (dbm) ligands and alkoxy substituents ($-\text{OR}$) were prepared [61], where $\text{R} = \text{C}_n\text{H}_{2n+1}$ and $n = 1, 2, 3, 5, 6, 12, 14, 16, 18$ (Figure 12). Fluorescence spectra and lifetimes were found to be nearly identical for dyes in CH_2Cl_2 solution; whereas, emission maxima and lifetimes were different among the samples in the solid state as powders, thin films, or spin cast films. The recovery time generally increased with alkyl chain length, ranging from minutes ($n = 3$) to days ($n = 18$). Longer chain analogues ($n = \frac{1}{4} 6, 12, 14, 16, 18$) did not fully return to the original annealed emissive state even after months on quartz, though the dynamics are substrate-dependent.

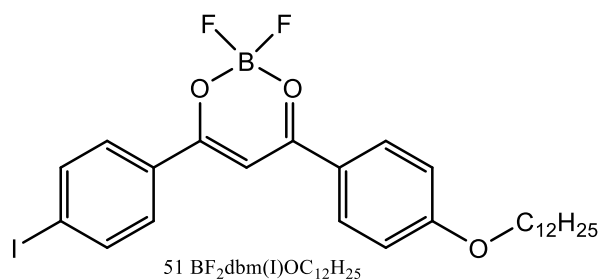


Figure 11. Structure of $\text{BF}_2\text{dbmOC}_{12}\text{H}_{25}$.

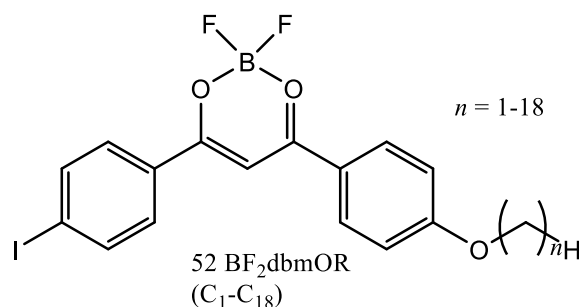


Figure 12. Structure of BF_2dbmOR .

The difluoroboron avobenzene complex (BF_2AVB) (Figure 13) is commercially available and used as an ingredient in sunscreen products because of its strong absorption of UVA light (320–400 nm) was synthesized via $\text{BF}_3 \cdot \text{OEt}_2$ boronation in CH_2Cl_2 avobenzene [62]. Unlike $\text{BF}_2\text{dbm}(\text{s})$ derivatives that typically exhibit strongly red-shifted and significantly broadened fluorescence spectra, $\text{BF}_2\text{AVB}(\text{s})$ showed unexpectedly sharp emission spectra that can be tuned via the solid form, such as single crystals, dendritic solid, or spin-cast film (Figure 14). The fluorescence color was found to be dramatically altered after crushing or physically smearing BF_2AVB crystals or upon scratching or rubbing annealed film samples.

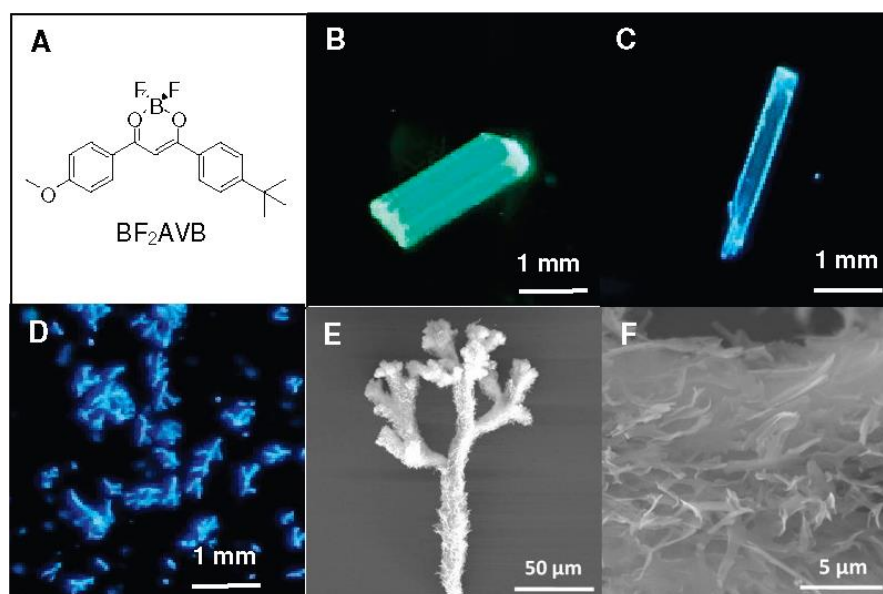


Figure 13. (A) Chemical structure of BF_2AVB . (B–D) Photos showing (B) green and (C) cyan crystals, and (D) the blue coral-like solid under UV excitation (λ_{ex} 365 nm). (E) SEM image of the dendritic coral-like structure. (F) Magnified view of the porous surface.

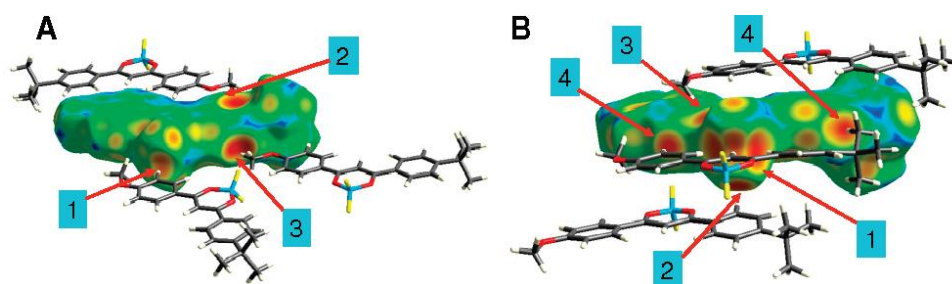


Figure 14. Crystal packing for (A) green and (B) cyan BF_2AVB crystals, showing Hirshfeld surfaces of the central molecules mapped with d_e . The most significant intermolecular interactions are as follows: (A1) C(arene)-H \cdots F hydrogen bond; (A2) C(methyl)-H $\cdots\pi$ interaction; (A3) short H \cdots H contacts; (B1, B2) C(arene)-H \cdots F hydrogen bonds; (B3) C(methyl)-H \cdots O hydrogen bond; (B4) short H \cdots H contacts.

The discovery of an exceptional group of boron-containing compounds, the borolithochromes, causing the distinct pink coloration of well-preserved specimens of the Jurassic red alga *Solenopora jurassica*, (Figure 15) was reported in [63]. The borolithochromes are characterized as complicated spiroborates (boric acid esters) with two phenolic moieties as boron ligands, representing a unique class of fossil organic pigments. Although the borolithochromes originated from a fossil red alga, no analogy with hitherto known present-day red algal pigments has been found. The occurrence of the borolithochromes or their possible digenetic products in the fossil record may provide additional information on the classification and phylogeny of fossil calcareous algae. Finally, boron measurements at sub-cellular scale are essential in boron neutron capture therapy (BNCT) of cancer as the nuclear localization of boron-10 atoms can enhance the effectiveness of killing individual tumor cells. Thus, the secondary ion mass spectrometry (SIMS)-based imaging technique of ion microscopy was used [64] to quantitatively image the boron from two BNCT agents, clinically using *p*-boronophenylalanine (BPA) and 3-carboranylthymidine(N4) (Figure 16) in mitotic metaphase and interphase human glioblastoma T98G cells. N4 belongs to a class of experimental BNCT agents, designated 3-carboranylthymidine analogues (3CTAs), which presumably accumulate selectively in cancer cells due to a process referred to as

kinase-mediated trapping (KMT). The cells were exposed to BPA for 1 h and N4 for 2 h. The BPA-treated interphase cells revealed significantly lower concentrations of boron in the perinuclear mitochondria-rich cytoplasmic region compared with the remaining cytoplasm and the nucleus, which were not significantly different from each other. In contrast, the BPA-treated metaphase cells revealed a significantly lower concentration of boron than cytoplasm in their chromosomes. In addition, the cytoplasm of metaphase cells contained significantly less boron than the cytoplasm of interphase cells.

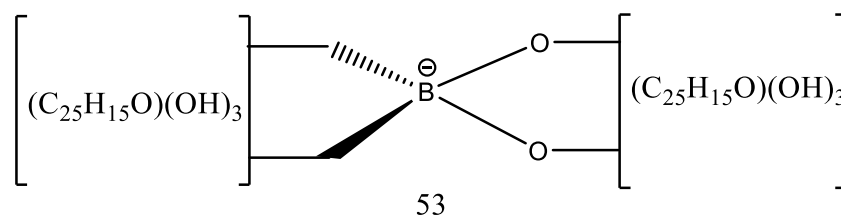


Figure 15. Structure of the main single isomeric borolithochrome ($C_{50}H_{36}O_{12}B$, [M] at m/z 839).

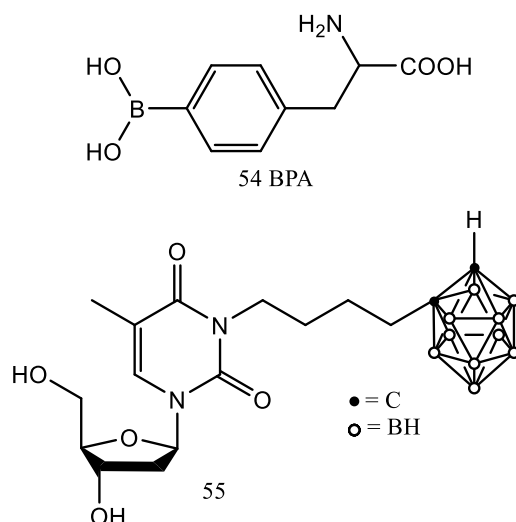
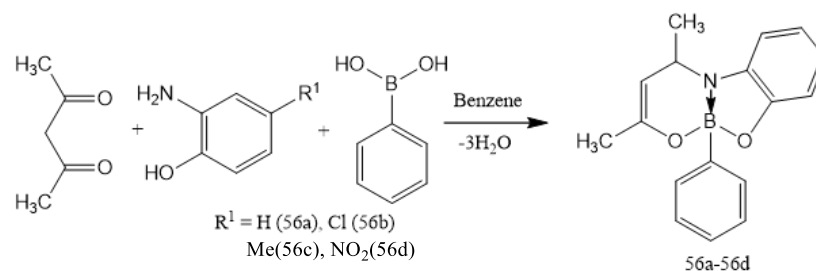


Figure 16. Chemical structures of boronophenylalanine and boronated nucleoside 55, 3-carboranylalkylthymidine.

4. O-B-N Boronates

A series of boronates **56a–56b** were synthesized by the single step reaction of 2,4-pentanedione, aminophenol, and phenylboronic acid in good yield (Scheme 11) [65]. The compounds crystallized in centrosymmetric space groups are useful for the growth of organic crystals with luminescent and nonlinear optical properties. The crystals were used to prepare aqueous colloidal nanocrystals that exhibited superior fluorescence properties to those of the boronates when dissolved in organic solvents. This image shows a photograph of the luminescence observed from the colloidal solution (Figure 17); for comparison, this figure also shows the absence of fluorescence from a chloroform solution of **56b** with the same molar concentration as the colloidal solution of nanocrystals.



Scheme 11. Synthesis of O-B-N Boronates **56a–56b** in one step from the reaction of 2,4-pentanedione, aminophenol, and phenylboronic acid.

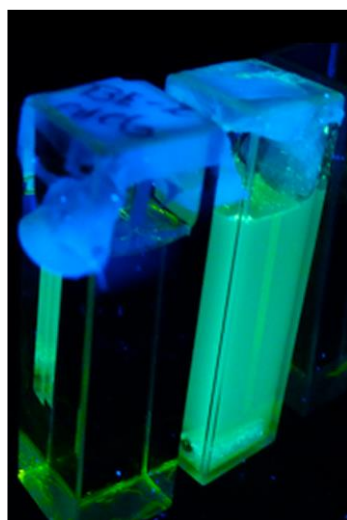
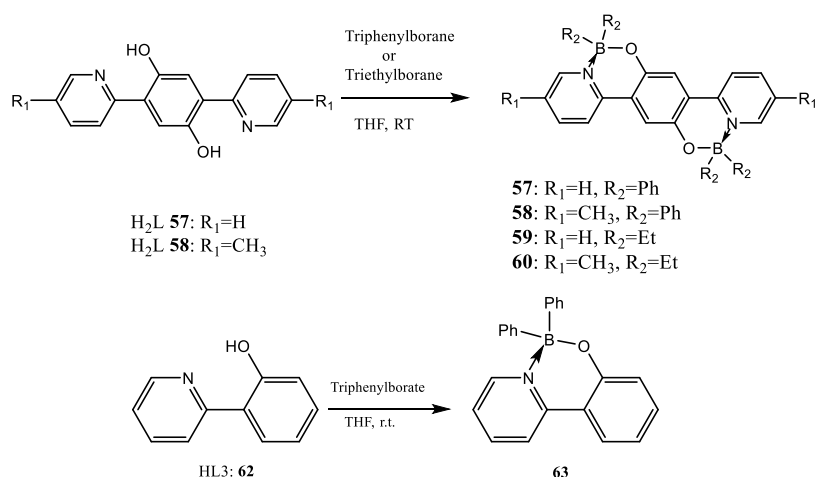


Figure 17. Photoluminescence from boronate **56b** in a chloroform solution (left in the picture) and from a colloidal solution of nanocrystals (right in the picture). Fluorescence was obtained under excitation at 370 nm.

N,O-containing bororganic compounds are also common [66]. Thus, four diboron-containing ladder-type π -conjugated compounds **57–60** (Scheme 12) were designed and synthesized [67]. Compounds **57** and **58** possess high thermal stabilities, moderate solid-state fluorescence quantum yields, as well as stable redox properties, indicating that they are possible candidates for emitters and charge-transporting materials in electroluminescent devices. The third-order nonlinear optical characterization of a boronate (**58**)—prepared from the reaction of diphenylboronic acid and the bidentate ligand (**57**)—derived from 4-dimethylaminocinnamaldehyde (Figure 18), was performed by third-harmonic generation (THG) at the infrared wavelength of 1550 nm [68]. The results showed that the N→B coordinative bond facilitates the polarization of the electronic π -system, a situation that optimizes the third-order nonlinear optical (NLO) response. In addition, three boron complexes (**65a–65c**) were prepared by the reaction of bidentate ligands (**66a–66c**) and diphenylboronic acid (Scheme 13) [69]. Compounds **58a** and **58c** were found to have a nonplanar conformation for the main p-backbone, acquired after boron complexation; for compound **58b**, the planar conformation is preserved.



Scheme 12. Synthesis of N,O-containing bororganic compounds 57–60.

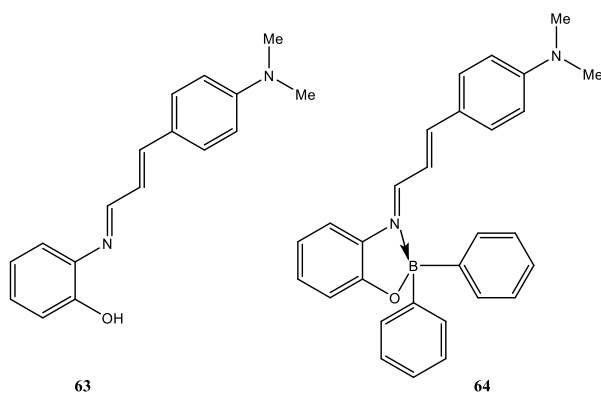
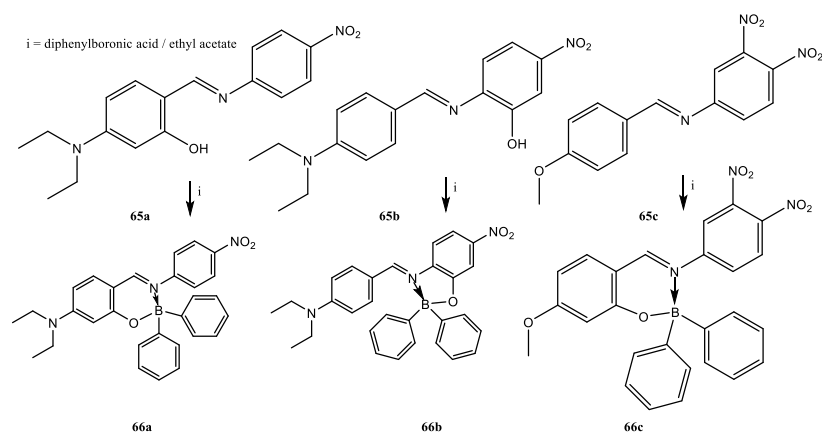


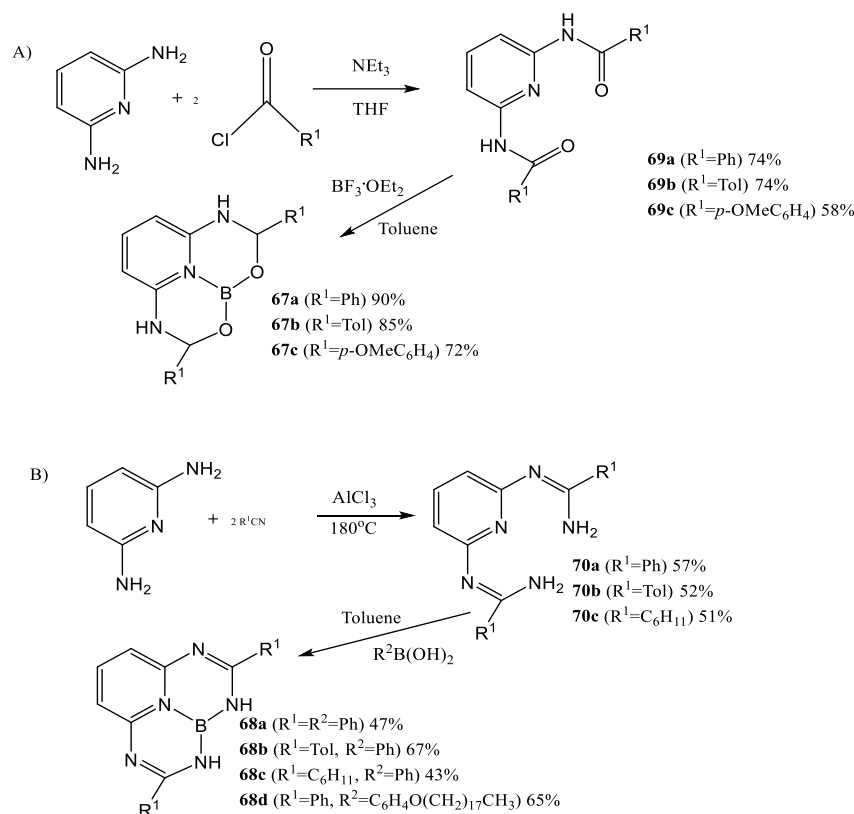
Figure 18. Structures of bidentate ligand (**63**) and boronate (**64**).



Scheme 13. Synthesis of **65a–65c** from **66a–66c** and diphenylborinic acid.

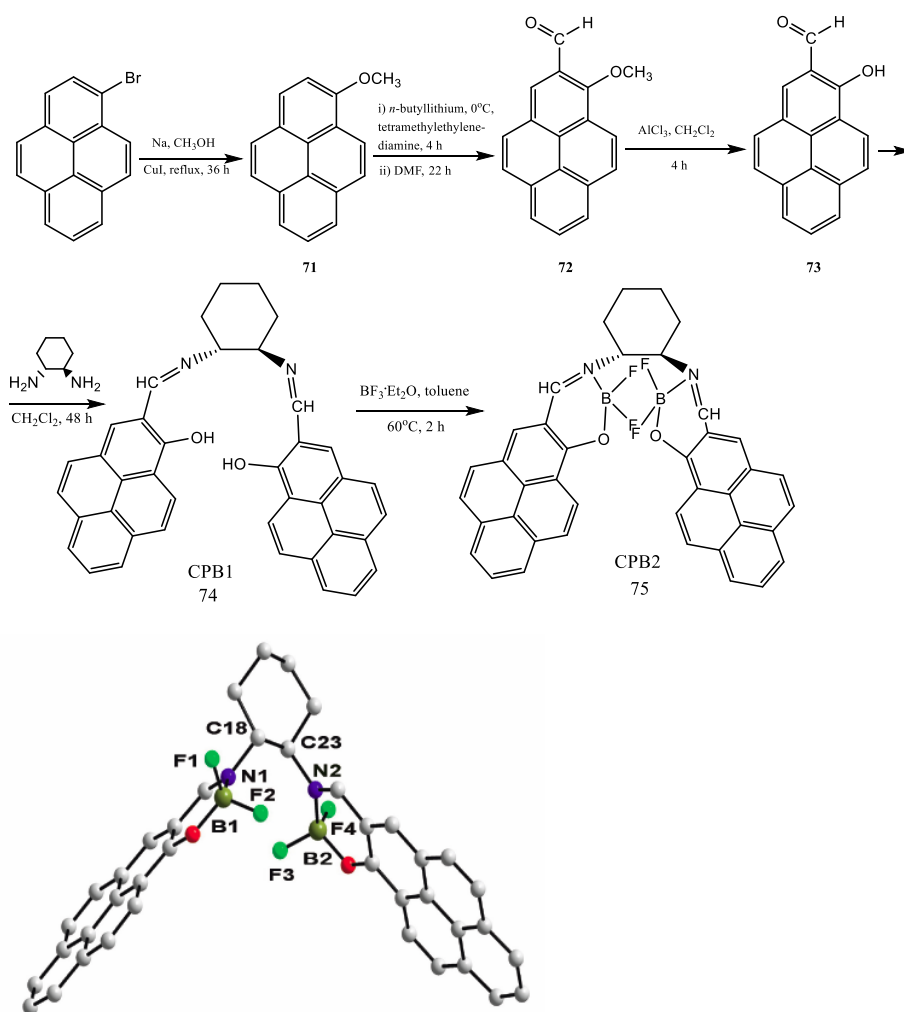
A series of fluorescent boron systems **67a–67c** and **68a–68d** based on nitrogen (NNN) or nitrogen and oxygen (ONO)-containing tridentate ligands were prepared (Scheme 14) [70]. They showed large Stokes shifts (mostly above 3200 cm^{-1}) and quantum yields in solution and in the solid state up to 40%. Introducing a long alkyl chain with a phenyl spacer at this axial position enables the self-assembly of the boron compound **68d** to form a fluorescent vesicle, which is able to encapsulate small molecules such as sulforhodamine. Additionally, boron compound **68d** was found to serve as a dye for cell imaging since it has the capability of binding to the nuclear membrane cells. A boron complex bearing a pyrene ligand

(CPB) as fluorophore was synthesized (Scheme 15) and introduced as the first example of a binuclear boron complex inorganic light-emitting diode [71]. Complex CPB exhibited strong red-light emission in the solid state. In the polymer light-emitting diodes fabricated with the CPB complex blended with PVK, red emission could be achieved easily by tuning the weight concentration of CPB.

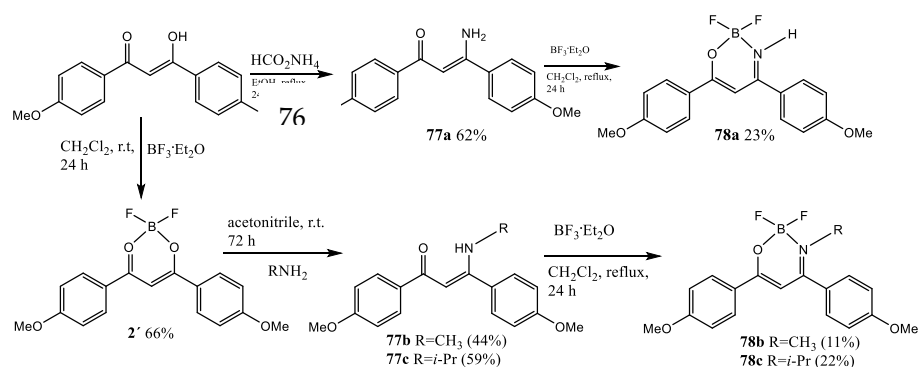


Scheme 14. Synthesis of boron complexes based on (A)ONO- and (B) NNN-tridentate ligands.

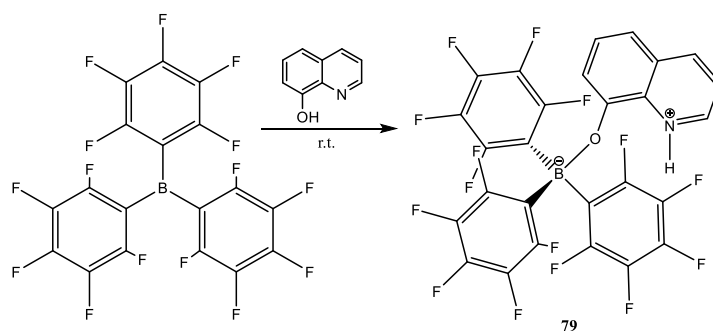
A series of boron ketoiminate derivatives that exhibited clear aggregation-induced emission (AIE) characteristics (in THF, FPL = 0.01; in the solid state, FPL = 0.30–0.76) were prepared by the reactions of 1,3-enaminoketone derivatives with boron trifluoride–diethyl etherate (Scheme 16) [72–83]. The boron ketoiminate units can be applied as a new building block of various AIE-active materials. The reaction of 8-hydroxyquinoline (HQ) with $\text{B}(\text{C}_6\text{F}_5)_3$ led [84–88] to the formation of the zwitterionic compound $(\text{C}_6\text{F}_5)_3\text{BQH}$ (Scheme 17). On the basis of these and other results, it was shown that fluorination of the phenyl rings results in a stabilization of both the HOMO and LUMO levels; therefore, the effect on the absorption and emission maxima in the UV–Vis and PL spectra, respectively, is only minimal. However, the difference in stability and volatility between fluorinated and unfluorinated luminescent boron compounds may have an effect on their solid-state properties and their performance in OLED devices.



Scheme 15. Synthetic route of the compound CPB and its crystal structure.



Scheme 16. Synthetic route to boron ketoiminate 78a–78c.



Scheme 17. Synthesis of $(C_6F_5)_3BQH$ with 8-hydroxyquinoline (HQ) and $B(C_6F_5)_3$.

Among benzoxazole and benzothiazole derivatives, two π -conjugated organoboron complexes **80** and **81** (Figure 19) with rigid seven-ring fused core structures bridged by boron atoms and highly efficient red (632 nm) and deep red (670 nm) solid-state fluorescence were constructed [89–94] (Scheme 18) and qualified as potential nondoped red emitters accompanied by excellent electron-transport ability. The two side phenyl groups coordinated to each boron atom effectively keep the luminescent units apart. As a result, these red fluorophores are brightly fluorescent in the solid state (fluorescence quantum yields: 0.30 for **80** and 0.41 for **81**). Their emission spectra are shown (Figure 20). 2-(20-Hydroxyphenyl)benzoxazole (HBO) and 2-(20-hydroxyphenyl)benzothiazole (HBT) reacted with triphenylborane produced two rigid p -conjugated fluorescent cores: **82** ($BPh_2(BOZ)$, BOZ 2-(benzo[d]oxazol-2-yl)phenol); **83** ($BPh_2(BTZ)$, BTZ 2-(benzo[d]thiazol-2-yl)phenol) [95–99]. Simple modification of these frameworks (Scheme 19) allowed the synthesis of strongly fluorescent materials **84** (BPh_2 (para-Cz-BTZ), Cz 9H-carbazol-9-yl), **85** (BPh_2 (para-NPh₂-BOZ), NPh₂diphenylamino), **86**, and **87** (BPh_2 (para-NMe₂-BTZ), NMe₂dimethylamino). Organic light-emitting diodes employing these boron complexes as emitters not only kept the full-color tunable emission feature but also showed high electroluminescent performance.

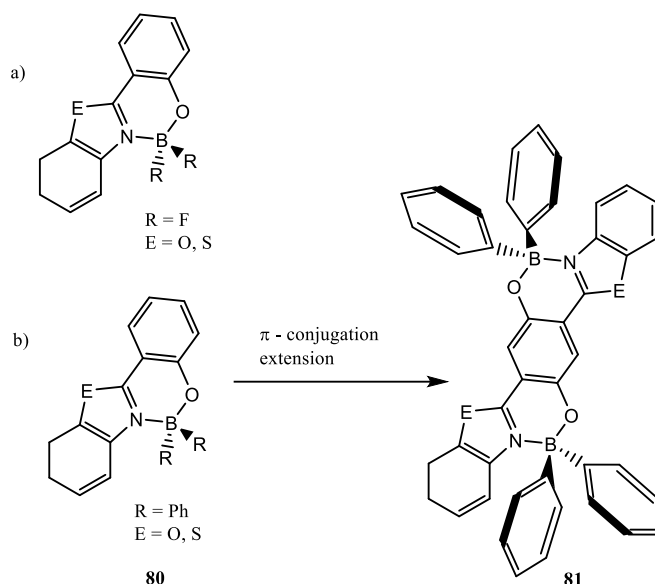
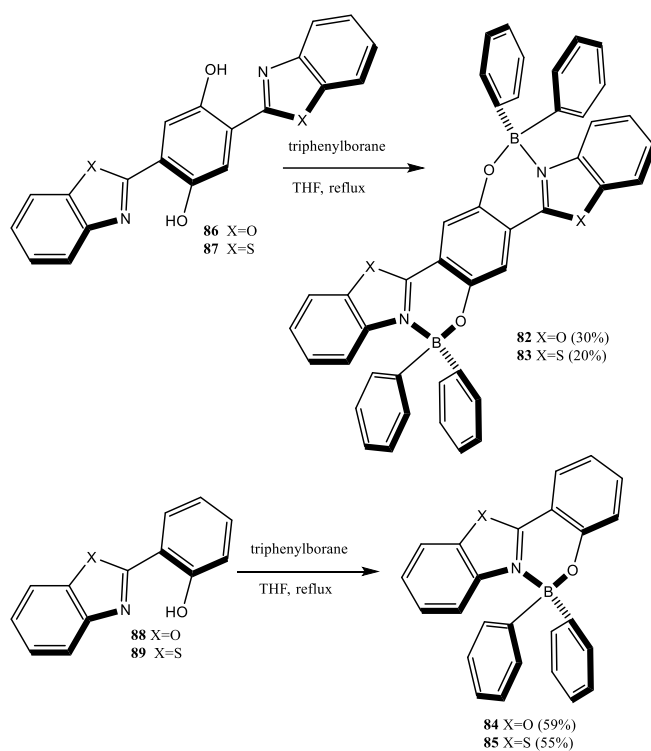
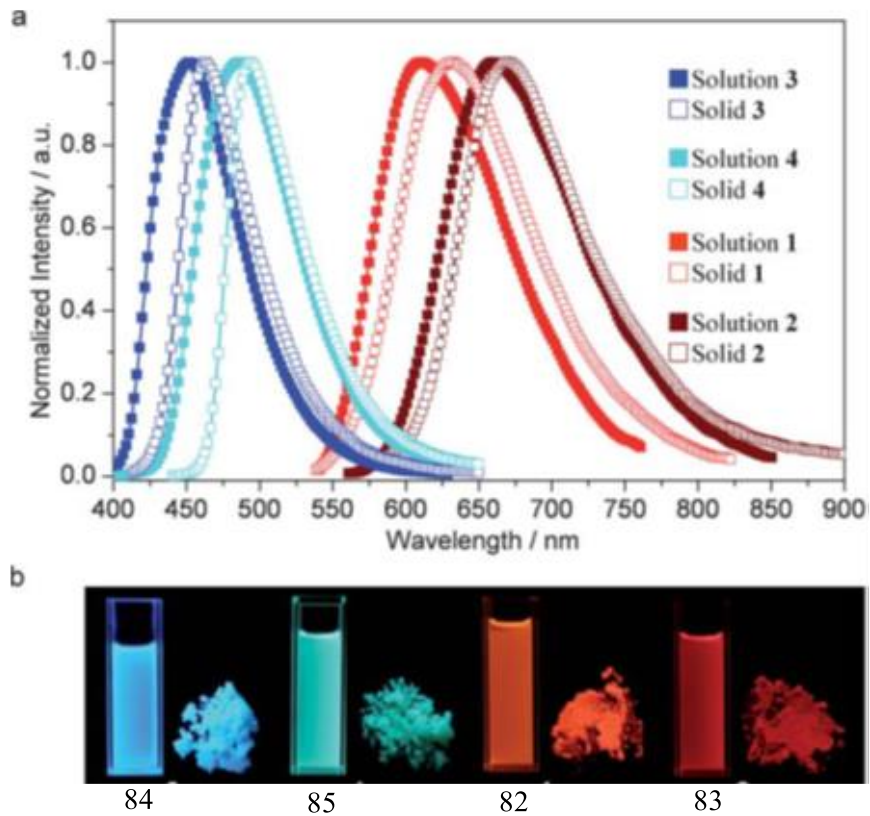
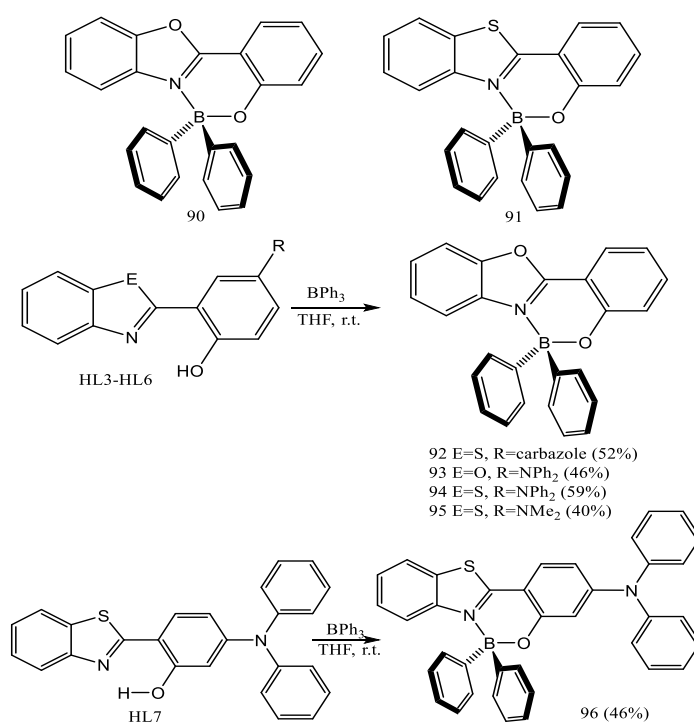


Figure 19. The design strategy towards diboron-containing complexes with a seven-ring fused π -conjugated skeleton (a) R = Fluorene based 2-(2'-hydroxyphenyl)benzoxazole and 2-(2'-hydroxyphenyl)benzothiazole ligands. (b) scheme of formation of fluorescent red and deep red boron containing complex.



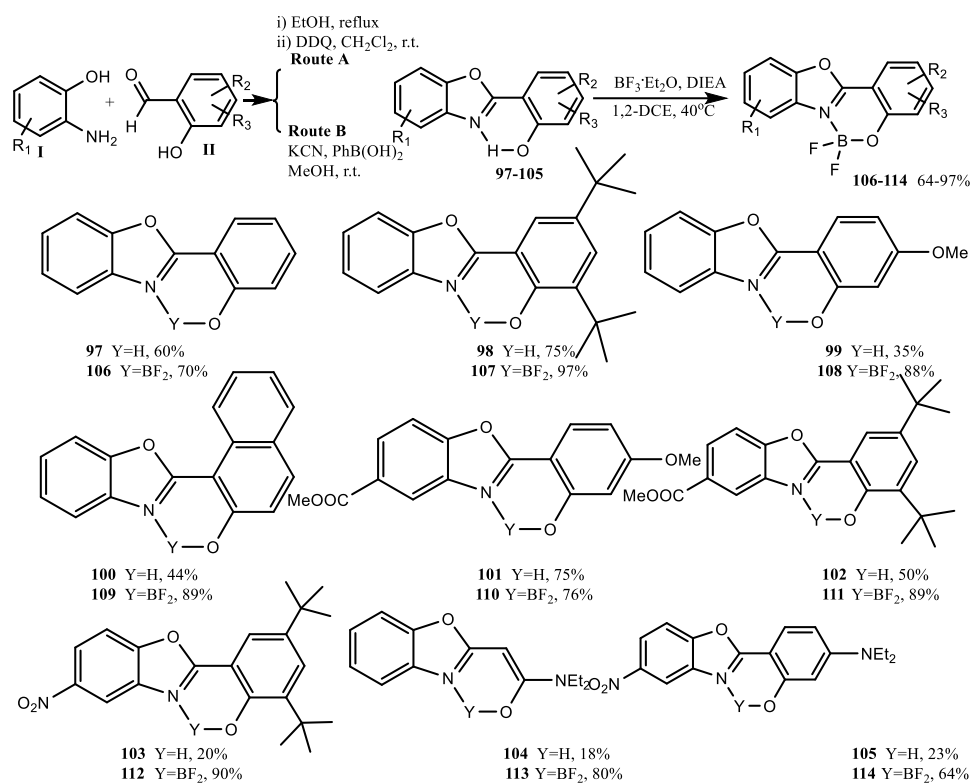
Scheme 18. Synthetic routes to the boron complexes 82–85.

Figure 20. Emission spectra (a) and photographs under UV light (365 nm) (b) of 82–85 in CH_2Cl_2 and the solid state.



Scheme 19. Molecular structures of complexes **91** and **92** and synthetic routes for complexes **93–96**.

Complexation of boron trifluoride by a series of electron donor/acceptor substituted 2-(20-hydroxy phenyl) benzoxazole (HBO) derivatives resulted in luminescent B(III) complexes **106–114** (Scheme 19) with an emission wavelength ranging from 385 to 425 nm in dichloromethane or toluene [100]. Depending on the nature of the substituents present on the core of the starting substituted 2-aminophenol I and 2-hydroxybenzaldehyde II, two different routes were chosen. Route A involved refluxing I and II together in ethanol to obtain the cyclic carbinolamines, which precipitated from the reaction mixture (Scheme 20). After collection, these compounds were oxidized with slight excess of 2,3-dichloro-5,6-dicyano-1,4-benzoquinone (DDQ). The second one-pot route B involves the oxidation-sensitive substituents, such as diethylamino groups, in presence of phenylboronic acid and requires potassium cyanide to promote benzoxazole cyclization. The synthesized dyes can be connected to other photoactive subunits such as BODIPY or Boranil cores to afford sophisticated molecular cassettes. In addition, four diboron-bridged, π -conjugated ladder molecules **115** were designed (Figure 21) and synthesized (Scheme 21) [101]. It was revealed that the bulky phenyl substituents on boron centers efficiently prevented π stacking of the luminescent ladder unit. The construction of diboron-containing ladder-type skeletons endowed these materials with good thermal stability, high fluorescence quantum yields, and strong electron affinity. Simple EL devices fabricated using complexes **116** and **117** as both emitter- and electron-transporting materials exhibited the highest brightness and efficiency among boron-containing materials reported so far. Finally, fluorescent homopolymers and amphiphilic block copolymers were prepared by reversible addition–fragmentation chain transfer (RAFT) polymerization of two styryl-type organoboron monomers (Scheme 22) [102–105]. Block copolymers featuring a relatively long PEO segment formed stable micellar solutions in water with luminescence characteristics similar to those of the respective (water-insoluble) homopolymers, suggesting potential applications as nanosized fluorophores in biological environments.



Scheme 20. Synthesis of substituted 2-(20-hydroxyphenyl)-benzoxazole (HBO) **97–105** derivatives and their corresponding B(III) complexes **106–114**.

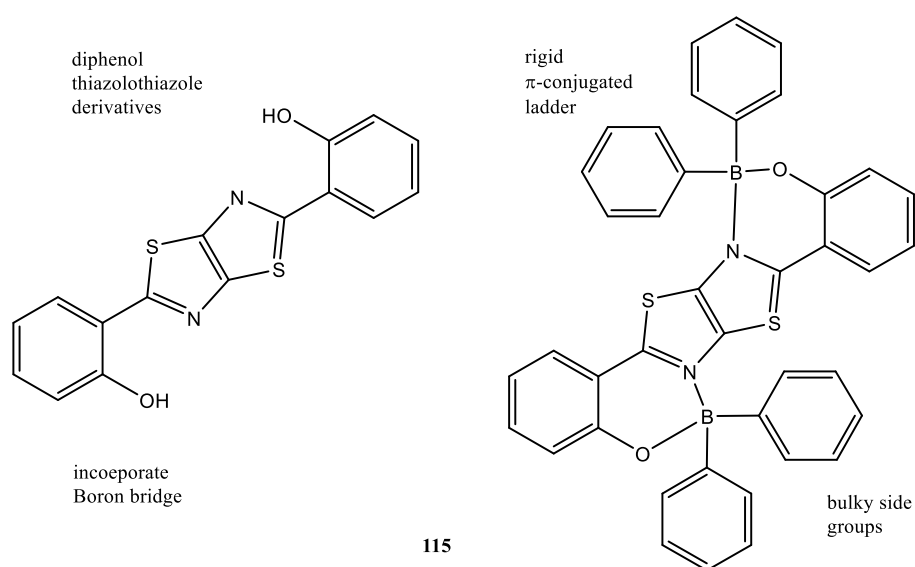
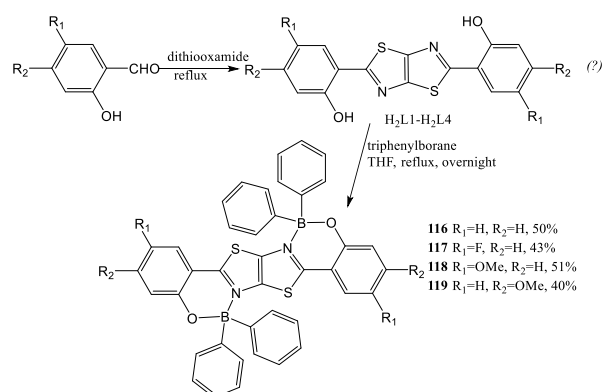
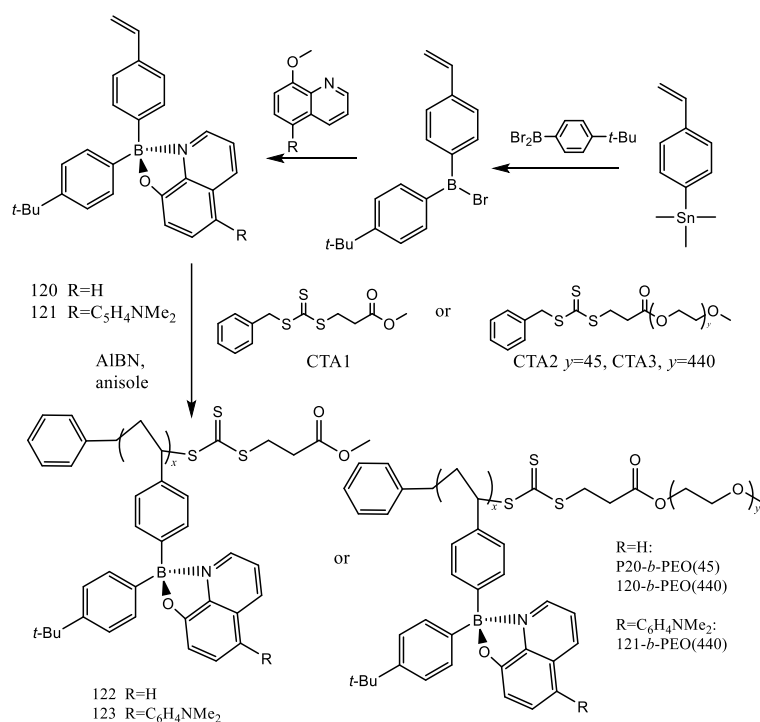


Figure 21. Design of a strategy toward a diboron-containing ladder **115**.



Scheme 21. Synthetic procedure for diboron complexes **116–119**.

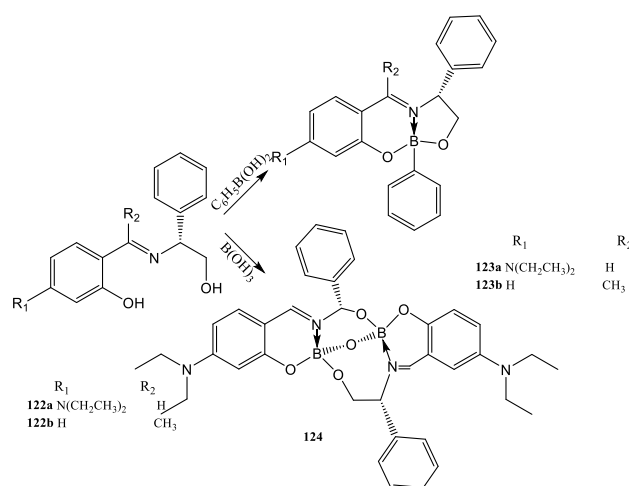


Scheme 22. Synthesis of organoboron quinolate monomers and polymers.

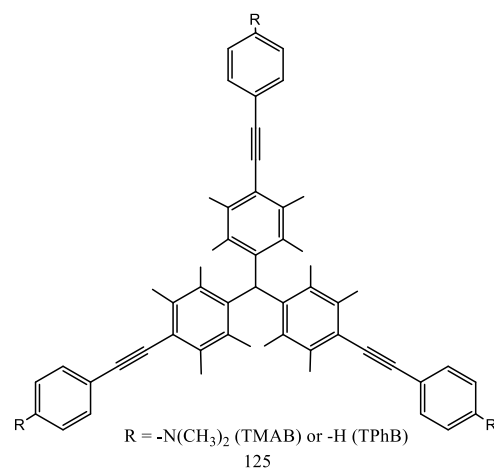
Among other interesting O-B-N-containing organoboron compounds are the so-called “push–pull” type of molecules [106–108]. These compounds derive from the well-known stilbene backbone, to which an arylboron (ArB) fragment has been added. This family of readily available macrocyclic boron compounds has recently attracted some interest from various perspectives in analytical and supramolecular chemistry. Thus, a series of eighteen such molecules were obtained by self-assembly of salicylideneimino phenols and various phenylboronic acids [109–114]. Such compounds can be prepared according to the reactions where a monomeric boronate and an oxobridged chiral dimer were obtained by reaction of the ligand derived from 4-diethylaminosalicylaldehyde with (R)-(R)-phenylglycinol and phenyl boronic acid or boric acid (Table 1) [115–121]. The existence of the N–B coordination bond was established by ¹¹BNMR, which showed the characteristic signal at 4.0, 2.1, and 6.1 ppm for **125**, **122a**, and **123b**, respectively (Scheme 23). Electric-field-induced second-harmonic measurements of the nonlinear optical response revealed that the nature of the phenyl-boron moieties has a modest influence on the molecular hyperpolarizabilities.

Table 1. Table for preparation of various salicylideniminophenols.

| Compound 1 | | | | | | Compound 2 | | | | | |
|----------------|----------------|-----------------|----------------|----------------|----------------|----------------|----------------|-----------------|----------------|----------------|----------------|
| R ₁ | R ₂ | R ₃ | R ₄ | R ₅ | R ₆ | R ₁ | R ₂ | R ₃ | R ₄ | R ₅ | R ₆ |
| OMe | H | H | H | H | H | 1a | H | H | H | H | H |
| | H | NO ₂ | H | H | H | 1b | H | NO ₂ | H | H | H |
| | F | F | F | F | F | 1c | F | F | F | F | F |
| | F | H | F | H | H | 1d | F | H | F | H | H |
| | H | Cl | H | H | H | 1e | H | Cl | H | H | H |
| | H | H | Cl | H | H | 1f | H | H | Cl | H | H |
| | H | H | Me | H | H | 1g | H | H | Me | H | H |
| | H | OMe | H | H | H | 1h | H | OMe | H | H | H |
| | | | | | | | H | H | Br | H | 2i |

**Scheme 23.** Synthesis of boronates **122a**, **123b**, and **124**.

Solvent effects on the spectroscopic and photophysical properties of tris{[*p*-(*N,N*-dimethylamino)phenylethynyl]-duryl}borane (TMAB) and tris[(phenylethynyl)duryl]borane (TPhB) (Figure 22) were studied [122–135]. Both TMAB and TPhB exhibited broad and structureless absorption and fluorescence bands attributed to the charge transfer (CT) transition between the π -orbital of the aryl group ($\pi(\text{aryl})$) and the vacant *p*-orbital on the boron atom (*p*(B)): $\pi(\text{aryl})$ -*p*(B) CT.

**Figure 22.** Structures of TMAB and TPhB.

5. Conclusions

In this review, we summarized various synthetic methods of BODIPY-based organoboron compounds with different frameworks. We also summarized the various optical and non-linear properties of these compounds along with their applications. BODIPY compounds based on NBN network were synthesized by Liebeskind–Srogl; Liebeskind–Srogl and Suzuki coupling showed intense absorption and large Stokes, unlike the typical BODIPY due to the geometry relaxation. The DFT calculations supported the geometrical relaxation upon photoexcitation and its remarkable effect on the energy levels of molecular orbitals. Moreover, boron compounds containing O-B-O- upon interaction with aggregates increase the fluorescence by 70-fold to 90 nm blue shift and significantly increase in quantum yield. New compounds such as the boron dodecane complex (BF₂dbmOC₁₂H₂₅) have emerged with dependent and reversible mechanochromic fluorescence.

A series of fluorescent boron systems based on nitrogen (NNN) or nitrogen and oxygen (ONO)-containing tridentate ligands were reported. They showed large Stokes shifts and quantum yields in solution and in the solid state. Introducing a long alkyl chain with a phenyl spacer at this axial position enables the self-assembly of the boron compound to form a fluorescent vesicle, which is able to encapsulate small molecules such as sulforhodamine. Furthermore, few boron compounds were found to serve as a dye for cell imaging since it has the capability of binding to the nuclear membrane cells. Moreover, a boron complex bearing a pyrene ligand (CPB) as fluorophore was synthesized and introduced as the first example of a binuclear boron complex inorganic light-emitting diode. Complex CPB exhibited strong red-light emission in the solid state. In the polymer light-emitting diodes fabricated with the CPB complex blended with PVK, red emission could be achieved easily by tuning the weight concentration of CPB.

Finally, fluorescent homopolymers and amphiphilic block copolymers were prepared by reversible addition–fragmentation chain transfer (RAFT) polymerization of two styryl-type organoboron monomers. Block copolymers featuring a relatively long PEO segment formed stable micellar solutions in water with luminescence characteristics similar to those of the respective homopolymers, suggesting potential applications as nanosized fluorophores in biological environments.

Author Contributions: Conceptualization, original draft preparation, review and editing and project administration P.M.G., V.M.J.P. and N.S.H.; investigation and resources, B.M.M.-F.; Formal analysis V.P.S.; All authors have read and agreed to the published version of the manuscript.

Funding: This research study was funded by the PAICYT (Grant: CE-1721-21), Chemistry Faculty-UANL for the financial support, VGST, Govt. of Karnataka for VGST-SMYSR (GRD 503), VGST KFIST L-1(GRD 952), RCU for Minor Research Project (2019 and 2020 respectively) and DST for DST-FIST grant.

Conflicts of Interest: The authors declare no conflict of interest.

Sample Availability: Samples of the compounds are not available from the authors.

References

1. James, T.D.; Shinkai, S. Saccharide-Selective Boronic Acid Based Photoinduced Electron Transfer (PET) Fluorescent Sensors. *Top. Curr. Chem.* **2002**, *218*, 159.
2. Jelinek, R.; Kolusheva, S. Carbohydrate biosensor. *Chem. Rev.* **2004**, *104*, 5987–6015. [[CrossRef](#)] [[PubMed](#)]
3. Pal, A.; Berube, M.; Hall, D.G. Design, Synthesis, and Screening of a Library of Peptidyl Bis(Boroxoles) as Oligosaccharide Receptors in Water: Identification of a Receptor for the Tumor Marker TF-Antigen Disaccharide. *Angew. Chem. Int. Ed.* **2010**, *49*, 1492–1495. [[CrossRef](#)] [[PubMed](#)]
4. Hansen, J.S.; Christensen, J.B.; Petersen, J.F.; Hoeg Jensen, T.; Norrild, J.C. Arylboronic acids: A diabetic eye on glucose sensing. *Sens. Actuators* **2012**, *B161*, 45–79. [[CrossRef](#)]
5. Wade, C.R.; Broomsgrove, A.J.; Aldridge, S.; Gabbai, F.P. Fluoride Ion Complexation and Sensing Using Organoboron Compounds. *Chem. Rev.* **2010**, *110*, 3958–3984. [[CrossRef](#)] [[PubMed](#)]
6. Wu, X.; Li, Z.; Chen, X.-X.; Fossey, J.S.; James, T.D.; Jiang, Y.B. Selective sensing of saccharides using simple boronic acids and their aggregates. *Chem. Soc. Rev.* **2013**, *42*, 8032–8048. [[CrossRef](#)] [[PubMed](#)]

7. Guan, Y.; Zhang, Y. Boronic acid-containing hydrogels: Synthesis and their applications. *Chem. Soc. Rev.* **2013**, *42*, 8106–8121. [[CrossRef](#)]
8. You, L.; Zha, D.; Anslyn, E.V. Recent Advances in Supramolecular Analytical Chemistry Using Optical Sensing. *Chem. Rev.* **2015**, *115*, 7840–7892. [[CrossRef](#)]
9. Wu, J.; Kwon, B.; Liu, W.; Anslyn, E.V.; Wang, P.; Kim, J.S. Chromogenic/Fluorogenic Ensemble Chemosensing Systems. *Chem. Rev.* **2015**, *115*, 7893–7943. [[CrossRef](#)]
10. Suzuki, A.; Brown, H.C. *Organic Syntheses Via Boranes*; Aldrich Chemical Company: Burlington, MA, USA; Milwaukee: Brookfield, WI, USA, 2003; Volume 3.
11. Hall, D.G. *Boronic Acids*, 2nd ed.; Wiley-VCH: Weinheim, Germany, 2011.
12. Gutekunst, W.R.; Baran, P.S. C–H functionalization logic in total synthesis. *Chem. Soc. Rev.* **2011**, *40*, 1976–1991. [[CrossRef](#)]
13. Chen, J.B.; Whiting, A. Recent Advances in Copper-Catalyzed Asymmetric Hydroboration of Electron-Deficient Alkenes: Methodologies and Mechanism. *Synthesis* **2018**, *50*, 3843–3861.
14. Collins, B.S.L.; Wilson, C.M.; Myers, E.L.; Aggarwal, V.K. Asymmetric Synthesis of Secondary and Tertiary Boronic Esters. *Angew. Chem. Int. Ed.* **2017**, *56*, 11700–11733. [[CrossRef](#)] [[PubMed](#)]
15. Crudden, C.M.; Edwards, D. Catalytic Asymmetric Hydroboration: Recent Advances and Applications in Carbon–Carbon Bond-Forming Reactions. *Eur. J. Org. Chem.* **2003**, *24*, 4695–4712. [[CrossRef](#)]
16. Waghorn, P.A.; Jones, M.W.; McIntyre, A.; Innocenti, A.; Vullo, D.; Harris, A.L.; Supuran, C.T.; Dilworth, J.R. Targeting Carbonic Anhydrases with Fluorescent BODIPY-Labelled Sulfonamides. *Eur. J. Inorg. Chem.* **2012**, *17*, 2898–2907. [[CrossRef](#)]
17. Porrès, L.; Mongin, O.; Desce, M.B. Synthesis, fluorescence and two-photon absorption properties of multichromophoric boron-dipyrrromethene fluorophores for two-photon-excited fluorescence applications. *Tetrahedron Lett.* **2006**, *47*, 1913–1917. [[CrossRef](#)]
18. Quan, L.; Chen, Y.; Lv, X.; Fu, W. Naphthyridine–BF₂ complexes with an amide-containing di-2-picolyamine receptor: Synthesis, structures and photo-induced electron transfer. *Chem. Eur. J.* **2013**, *272*, 73–79.
19. Karotki, A.; Khurana, M.; Lepock, J.R.; Wilson, B.C. Simultaneous Two-photon Excitation of Photofrin in Relation to Photodynamic Therapy. *Photochem. Photobiol.* **2006**, *82*, 443–452. [[CrossRef](#)] [[PubMed](#)]
20. Belfield, K.D.; Corredor, C.C.; Morales, A.R.; Dessources, M.A.; Hernandez, F.E. Synthesis and Characterization of New Fluorene-Based Singlet Oxygen Sensitizers. *J. Fluoresc.* **2006**, *16*, 105–110. [[CrossRef](#)]
21. Oar, M.A.; Serin, J.M.; Dichtel, W.R.; Frechet, J.M.J.; Ohulchanskyy, T.Y.; Prasad, P.N. Photosensitization of Singlet Oxygen via Two-Photon-Excited Fluorescence Resonance Energy Transfer in a Water-Soluble Dendrimer. *Chem. Mater.* **2005**, *17*, 2267–2275. [[CrossRef](#)]
22. Fournier, M.; Pepin, C.; Houde, D.; Ouellet, R.; Van Lier, J.E. Ultrafast studies of the excited-state dynamics of copper and nickel phthalocyanine tetrasulfonates: Potential sensitizers for the two-photon photodynamic therapy of tumors. *Photochem. Photobiol. Sci.* **2004**, *3*, 120–126. [[CrossRef](#)]
23. Kubota, Y.; Hara, H.; Tanaka, S.; Funabiki, K.; Matsui, M. Synthesis and Fluorescence Properties of Novel Pyrazine–Boron Complexes Bearing a β -Iminoketone Ligand. *Org. Lett.* **2011**, *13*, 6544–6547. [[CrossRef](#)] [[PubMed](#)]
24. Araneda, J.F.; Piers, W.E.; Heyne, B.; Parvez, M.; McDonald, R. BiO(IO₃): A New Polar Iodate that Exhibits an Aurivillius-Type (Bi₂O₂)²⁺ Layer and a Large SHG Response. *Angew. Chem.* **2011**, *123*, 12422–12425. [[CrossRef](#)]
25. Bouit, P.A.; Wetzell, G.; Berginc, G.; Loiseaux, B.; Toupet, L.; Feneyrou, P.; Bretonniere, Y.; Kamada, K.; Maury, O.; Andraud, C. Near IR Nonlinear Absorbing Chromophores with Optical Limiting Properties at Telecommunication Wavelengths. *Chem. Mater.* **2007**, *19*, 5325–5335. [[CrossRef](#)]
26. Guyen, L.H.; Straub, M.; Gu, M. Acrylate-Based Photopolymer for Two-Photon Microfabrication and Photonic Applications. *Adv. Funct. Mater.* **2005**, *15*, 209–216.
27. Oenjarts, C.A.; Ober, C.K. Two-Photon Three-Dimensional Microfabrication of Poly(Dimethylsiloxane) Elastomers. *Chem. Mater.* **2004**, *16*, 5556–5558. [[CrossRef](#)]
28. Ehrlich, J.E.; Wu, X.L.; Lee, I.-Y.S.; Hu, Z.-Y.; Rockel, H.; Marder, S.R.; Perry, J.W. Two-photon absorption and broadband optical limiting with bis-donor stilbenes. *Opt. Lett.* **1997**, *22*, 1843–1845. [[CrossRef](#)] [[PubMed](#)]
29. Liebeskind, L.S.; Srogl, J. Thiol Ester–Boronic Acid Coupling. A Mechanistically Unprecedented and General Ketone Synthesis. *Am. Chem. Soc.* **2000**, *122*, 11260–11261. [[CrossRef](#)]
30. Peça-Cabrera, E.; Aguilar-Aguilar, A.; Gonzalez-Dominguez, M.; Lager, E.; Zamudio-Vazquez, R.; Godoy-Vargas, J.; Villanueva-Garcia, F. Simple, General, and Efficient Synthesis of Meso-Substituted Borondipyrrromethenes from a Single Platform. *Org. Lett.* **2007**, *9*, 3985–3988. [[CrossRef](#)] [[PubMed](#)]
31. Lager, E.; Liu, J.Z.; Aguilar-Aguilar, A.; Tang, B.Z.; Peça-Cabrera, E. Novel meso-Polyarylamine-BODIPY Hybrids: Synthesis and Study of Their Optical Properties. *J. Org. Chem.* **2009**, *74*, 2053–2058. [[CrossRef](#)] [[PubMed](#)]
32. Han, J.Y.; Gonzalez, O.; Aguilar-Aguilar, A.; Peça-Cabrera, E.; Burgess, K. 3- and 5-Functionalized BODIPYs via the Liebeskind-Srogl reaction. *Org. Biomol. Chem.* **2009**, *7*, 34–36. [[CrossRef](#)] [[PubMed](#)]
33. Arroyo, I.J.; Hu, R.R.; Tang, B.Z.; Lopez, F.I.; Peça-Cabrera, E. 8-Alkenylborondipyrrromethene dyes. General synthesis, optical properties, and preliminary study of their reactivity. *Tetrahedron* **2011**, *67*, 7244–7250. [[CrossRef](#)]

34. Roacho, R.I.; MettaMagana, A.J.; PeÇa-Cabrera, E.; Pannell, K.H. Synthesis, structural characterization, and spectroscopic properties of the *ortho*, *meta*, and *para* isomers of 8-(HOCH₂-C₆H₄)-BODIPY and 8-(MeOC₆H₄)-BODIPY. *J. Phys. Org. Chem.* **2013**, *26*, 345–351. [[CrossRef](#)]
35. Martinez-Gonzalez, M.R.; Urias-Benavides, A.; AlvaradoMartinez, E.; Lopez, J.C.; Gjmez, A.M.; del Rio, M.; Garcia, I.; Costela, A.; BaÇuelos, J.; Arbeloa, T.; et al. Convenient Access to Carbohydrate–BODIPY Hybrids by Two Complementary Methods Involving One-Pot Assembly of “Clickable” BODIPY Dyes. *Eur. J. Org. Chem.* **2014**, *2014*, 5659–5663. [[CrossRef](#)]
36. Karolin, J.; Johansson, B.A.L.; Strandberg, J.L.; NyZ, T. Fluorescence and Absorption Spectroscopic Properties of Dipyrrometheneboron Difluoride (BODIPY) Derivatives in Liquids, Lipid Membranes, and Proteins. *J. Am. Chem. Soc.* **1994**, *116*, 7801–7806. [[CrossRef](#)]
37. Loudet, A.; Burgess, K. BODIPY Dyes and Their Derivatives: Syntheses and Spectroscopic Properties. *Chem. Rev.* **2007**, *107*, 4891–4932. [[CrossRef](#)] [[PubMed](#)]
38. Leen, V.; Miscoria, D.; Yin, S.; Filarowski, A.; Ngongo, J.M.; Auweraer, M.V.; Boens, N.; Dehaen, W. 1,7-Disubstituted Boron Dipyrromethene (BODIPY) Dyes: Synthesis and Spectroscopic Properties. *J. Org. Chem.* **2011**, *76*, 8168–8176. [[CrossRef](#)]
39. Chen, Y.; Zhao, J.; Guo, H.; Xie, L. Geometry Relaxation-Induced Large Stokes Shift in Red-Emitting Borondipyrromethenes (BODIPY) and Applications in Fluorescent Thiol Probes. *J. Org. Chem.* **2012**, *77*, 2192–2206. [[CrossRef](#)]
40. Lakowicz, J.R. *Principles of Fluorescence Spectroscopy*, 2nd ed.; Kluwer Academic: New York, NY, USA, 1999.
41. Valeur, B. *Molecular Fluorescence: Principles and Applications*; Wiley-VCH Verlag: Weinheim, Germany, 2001.
42. Chibani, S.; LeGuennic, B.; Charaf-Eddin, A.; Maury, O.; Andraud, C.; Jacquemin, D. On the computational of asiabatic energies in aza-boron-dipyrromethene dyes. *Chem. Rev.* **2012**, *8*, 3303–3313.
43. Küköz, B.; Hayvalı, K.; Yılmaz, M.; U˘guz, H.; Ulas, B.; Kürüm, U.; Gul Yaglioglu, H.; Elmali, A. Synthesis, optical properties and ultrafast dynamics of aza-boron-dipyrromethene compounds containing methoxy and hydroxy groups and two-photon absorption cross-section. *J. Photochem. Photobiol. A Chem.* **2012**, *247*, 24–29. [[CrossRef](#)]
44. Liu, Y.; Kong, M.; Zhang, Z.; Zhou, H.; Zhang, S.; Li, S.; Wu, J.; Tian, Y. A series of triphenylamine-based two-photon absorbing materials with AIE property for biological imaging. *J. Mater. Chem. B* **2014**, *2*, 5430–5440. [[CrossRef](#)]
45. Du, M.L.; Hu, C.Y.; Wang, L.F.; Li, C.; Han, Y.Y.; Gan, X.; Chen, Y.; Mu, W.H.; Huang, M.L.; Fu, W.F. New members of fluorescent 1,8-naphthyridine-based BF₂ compounds: Selective binding of BF₂ with terminal bidentate N˘N˘O and N˘C˘O groups and tunable spectroscopy properties. *Dalton Trans.* **2014**, *43*, 13924–13931. [[CrossRef](#)] [[PubMed](#)]
46. Aranedá, J.F.; Piers, W.E.; Heyne, B.; Parvez, M.; McDonald, R. Progress in the Science of Functional Dyes. *Angew. Chem. Int. Ed.* **2011**, *50*, 1–5.
47. Wang, Y.; Zhang, D.; Zhou, H.; Ding, J.; Chen, Q.; Xiao, Y.; Qian, S. Nonlinear optical properties and ultrafast dynamics of three novel boradiazaindacene derivatives. *J. Appl. Phys.* **2010**, *8*, 33–520. [[CrossRef](#)]
48. Kowada, T.; Yamaguchi, S.; Ohe, K. Highly Fluorescent BODIPY Dyes Modulated with Spirofluorene Moieties. *Org. Lett.* **2010**, *12*, 296–299. [[CrossRef](#)]
49. Matthew, T.W.; Patel, N.M.; Roberts, S.T.; Kathryn, A.; Djurovich, I.P.; Bradforth, E.S.; Thompson, M.E. Symmetry-breaking intramolecular charge transfer in the excited state of *meso*-linked BODIPY dyads. *Chem. Commun.* **2012**, *48*, 284–286.
50. Li, Z.; Lin, T.; Liu, S.; Huang, C.; Hudnall, T.W.; Gabbai, F.P.; Conti, P.S. Rapid aqueous [¹⁸F]-labeling of a bodipy dye for positron emission tomography/fluorescence dual modality imaging. *Chem. Commun.* **2011**, *47*, 9324–9326. [[CrossRef](#)]
51. Kim, T.; Park, J.; Park, S.; Choi, Y.; Kim, Y. Visualization of tyrosinase activity in melanoma cells by a BODIPY-based fluorescent probe. *Chem. Commun.* **2011**, *47*, 12640–12642. [[CrossRef](#)]
52. Tokoro, Y.; Nagai, A.; Chujo, Y. Luminescent chiral organoboron 8-aminoquinolate-coordination polymers. *Appl. Organomet. Chem.* **2010**, *24*, 563–568. [[CrossRef](#)]
53. Tsunemasa, N.; Tsuboi, A.; Okamura, H. Effects of Organoboron Antifoulants on Oyster and Sea Urchin Embryo Development. *Int. J. Mol. Sci.* **2013**, *14*, 421–433. [[CrossRef](#)]
54. Martens, S.C.; Riehm, T.; Wadepohl, H.; Gade, L.H. Tetra-*N*-silylated Bis(borylene)tetraaminoperylene (“DIBOTAPs”): Synthesis, Structures and Photophysics. *Eur. J. Inorg. Chem.* **2012**, *18*, 3039–3046. [[CrossRef](#)]
55. Bolze, F.; Hayek, A.; Sun, X.H.; Baldeck, P.L.; Bourgogne, C.; Nicoud, J.-F. New insight in boron chemistry: Application in two-photon absorption. *Opt. Mater.* **2011**, *33*, 1453–1458. [[CrossRef](#)]
56. Mirochnik, A.G.; Fedorenko, E.V.; Gizzatulina, D.K.; Karasev, V.E. Photoinduced enhancement of luminescence from (dibenzoyl-methanato)boron difluoride in polymethyl methacrylate. *Russ. J. Phys. Chem.* **2007**, *81*, 1880–1883. [[CrossRef](#)]
57. Ran, C.; Xu, X.; Raymond, S.B.; Ferrara, B.J.; Neal, K.; Bacskai, B.J.; Medarova, Z.; Moore, A. Design, Synthesis, and Testing of Difluoroboron-Derivatized Curcumins as Near-Infrared Probes for in Vivo Detection of Amyloid-β Deposits. *J. Am. Chem. Soc.* **2009**, *131*, 15257–15261. [[CrossRef](#)] [[PubMed](#)]
58. Zhang, G.; Singer, J.P.; Kooi, S.E.; Evans, R.E.; Thomas, E.L.; Fraser, C.L. Reversible solid-state mechanochromic fluorescence from a boron lipid dye. *J. Mater. Chem.* **2011**, *21*, 8295. [[CrossRef](#)]
59. Zhang, G.; Lu, J.; Sabat, M.; Fraser, C.L. Polymorphism and Reversible Mechanochromic Luminescence for Solid-State Difluoroboron Avobenzene. *J. Am. Chem. Soc.* **2010**, *132*, 2160–2162. [[CrossRef](#)]
60. Nguyen, N.D.; Zhang, G.; Lu, J.; Sherman, A.E.; Fraser, C.L. Alkyl chain length effects on solid-state difluoroboron β-diketone mechanochromic luminescence. *J. Mater. Chem.* **2011**, *21*, 8409. [[CrossRef](#)]

61. Wang, Z.; Wang, M.; Peng, J.; Xie, Y.; Liu, M.; Gao, W.; Zhou, Y.; Huang, X.; Wu, H. Polymorphism and multicolor mechanofluorochromism of a D- π -A asymmetric 4H-pyran derivative with aggregation-induced emission property. *J. Phys. Chem.* **2019**, *123*, 27742–27751.
62. Wolkenstein, K.; Gross, J.H.; Falk, H. Boron-containing organic pigments from a Jurassic red alga. *Proc. Natl. Acad. Sci. USA* **2010**, *107*, 19374–19378. [[CrossRef](#)]
63. Chandra, S.; Tjarks, W.; Loreyand, D.R.; Barth, R.F. Quantitative subcellular imaging of boron compounds in individual mitotic and interphase human glioblastoma cells with imaging secondary ion mass spectrometry (SIMS). *J. Microsc.* **2008**, *229*, 92–103. [[CrossRef](#)]
64. Rodríguez, M.; Ramos-Ortíz, G.; Martha, I.; Alcalá-Salas, M.I.; Maldonado, J.L.; López-Varela, K.; López, Y.; Domínguez, O.; Meneses-Nava, M.A.; Barbosa-García, O.; et al. One-pot synthesis and characterization of novel boronates for the growth of single crystals with nonlinear optical properties. *Dyes Pigments* **2010**, *87*, 76–83. [[CrossRef](#)]
65. He, Z.; Trinchera, P.; Adachi, S.; Denis, J.D.S.; Andrei, K.; Yudin, K.A. Oxidative geminal functionalization of organoboron compounds. *Chem. Int. Ed.* **2012**, *51*, 11092–11096. [[CrossRef](#)] [[PubMed](#)]
66. Zhang, Z.; Bi, H.; Zhang, Y.; Yao, D.; Gao, H.; Fan, Y.; Zhang, H.; Wang, Y.; Wang, Y.; Chen, Z.; et al. Luminescent Boron-Contained Ladder-Type π -Conjugated Compounds. *ACS Inorg. Chem.* **2009**, *48*, 7230–7236. [[CrossRef](#)] [[PubMed](#)]
67. Rodríguez, M.; Castro-Beltrán, R.; Ramos-Ortiz, G.; Maldonado, J.L.; Farfan, N.; Domínguez, O.; Rodríguez, J.; Santillan, R.; Meneses-Nava, M.A.; Barbosa-García, O.; et al. Synthesis and third-order nonlinear optical studies of a novel four-coordinated organoboron derivative and a bidentate ligand: The effect of the N \rightarrow B coordinative bond. *Synth. Met.* **2009**, *159*, 1281–1287. [[CrossRef](#)]
68. Rodríguez, M.; Maldonado, J.L.; Ramos-Ortíz, G.; Domínguez, O.; Ochoa, M.E.; Santillan, R.; Farfán, N.; Meneses-Nava, M.; Barbosa-García, O. Synthesis, X-ray diffraction analysis, and chemical–optical characterizations of boron complexes from bidentate ligands. *Polyhedron* **2012**, *43*, 194–200. [[CrossRef](#)]
69. Glotzbach, C.; Kauscher, U.; Voskuhl, J.; SedaKehr, N.; Stuart, M.C.A.; Fröhlich, R.; Galla, H.J.; Ravoo, B.J.; Nagura, K.; Saito, S.; et al. Fluorescent Modular Boron Systems Based on NNN- and ONO-Tridentate Ligands: Self-Assembly and Cell Imaging. *J. Org. Chem.* **2013**, *78*, 4410–4418. [[CrossRef](#)] [[PubMed](#)]
70. Zhou, Y.; Kim, J.; Kim, M.J.; Son, W.; Han, S.J.; Kim, H.N.; Han, S.; Kim, Y.; Lee, C.; Kim, S.; et al. Novel Bi-Nuclear Boron Complex with Pyrene Ligand: Red-Light Emitting as well as Electron Transporting Material in Organic Light-Emitting Diodes. *Org. Lett.* **2010**, *12*, 1272–1275. [[CrossRef](#)]
71. Yoshii, R.; Nagai, A.; Tanaka, K.; Chujo, Y. Highly Emissive Boron Ketoiminate Derivatives as a New Class of Aggregation-Induced Emission Fluorophores. *Chem. Eur. J.* **2013**, *19*, 4506–4512. [[CrossRef](#)]
72. Tang, C.W.; VanSlyke, S.A. Organic electroluminescent diodes. *Appl. Phys. Lett.* **1987**, *51*, 913–915. [[CrossRef](#)]
73. Friend, R.H.; Gymer, R.W.; Holmes, A.B.; Burroughes, J.H.; Marks, R.N.; Taliani, C.; Bradley, D.D.C.; Dos Santos, D.A.; Brdas, J.L.; Lögdlund, M.; et al. Electroluminescence in conjugated polymers. *Nature* **1999**, *397*, 121–128. [[CrossRef](#)]
74. Jenekhe, S.A.; Osaheni, J.A. Excimers and Exciplexes of Conjugated Polymers. *Science* **1994**, *265*, 765–768. [[CrossRef](#)]
75. Luo, J.; Xie, Z.; Lam, J.W.Y.; Cheng, L.; Chen, H.; Qiu, C.; Kwok, H.S.; Zhan, X.; Liu, Y.; Zhu, D.; et al. Aggregation-induced emission of 1-methyl-1,2,3,4,5-pentaphenylsilole. *Chem. Commun.* **2001**, *18*, 1740–1741. [[CrossRef](#)] [[PubMed](#)]
76. Chen, J.; Law, C.C.W.; Lam, J.W.Y.; Dong, Y.; Lo, S.M.F.; Williams, I.D.; Zhu, D.; Tang, B.Z. Synthesis, Light Emission, Nanoaggregation, and Restricted Intramolecular Rotation of 1,1-Substituted 2,3,4,5-Tetraphenylsiloles. *Chem. Mater.* **2003**, *15*, 1535–1546. [[CrossRef](#)]
77. Chen, J.; Xie, Z.; Lam, J.W.Y.; Law, C.C.W.; Tang, B.Z. Silole-Containing Polyacetylenes. Synthesis, Thermal Stability, Light Emission, Nanodimensional Aggregation, and Restricted Intramolecular Rotation. *Macromolecules* **2003**, *36*, 1108–1117. [[CrossRef](#)]
78. Chen, J.; Xu, B.; Ouyang, X.; Tang, B.Z.; Cao, Y. Aggregation-Induced Emission of *cis*, *cis*-1,2,3,4-Tetraphenylbutadiene from Restricted Intramolecular Rotation. *J. Phys. Chem. A* **2004**, *108*, 7522–7526. [[CrossRef](#)]
79. Tong, H.; Dong, Y.Q.; Hußler, M.; Lam, J.W.Y.; Sung, H.H.Y.; Williams, I.D.; Sun, J.Z.; Tang, B.Z. Tunable aggregation-induced emission of diphenyldibenzofulvenes. *Chem. Commun.* **2006**, *10*, 1133–1135. [[CrossRef](#)]
80. Tong, H.; Hong, Y.; Dong, Y.; Hußler, M.; Lam, J.W.Y.; Guo, Z.; Li, Z.; Tang, B.Z. Fluorescent “light-up” bioprobes based on tetraphenylethylene derivatives with aggregation-induced emission characteristics. *Chem. Commun.* **2006**, *35*, 3705–3707. [[CrossRef](#)]
81. Zeng, Q.; Li, Z.; Dong, Y.; Di, Q.; Qin, A.; Hong, Y.; Zhu, J.; Zhu, Z.; Jim, C.K.W.; Yu, G.; et al. Fluorescence enhancements of benzene-cored luminophors by restricted intramolecular rotations: AIE and AIEE effects. *Chem. Commun.* **2007**, *1*, 70–72. [[CrossRef](#)]
82. Hong, Y.; Lam, J.W.Y.; Tang, B.Z. Aggregation-induced emission: Phenomenon, mechanism and applications. *Chem. Commun.* **2009**, *29*, 4332–4353. [[CrossRef](#)]
83. Hellstrom, J.S.; Britovsek, G.J.P.; Jones, T.S.; Hunt, P.; White, A.J.P. Synthesis and characterisation of luminescent fluorinated organoboron compounds. *Dalton Trans.* **2007**, *14*, 1425–1432. [[CrossRef](#)]
84. Mullen, K.; Scherf, U. (Eds.) *Organic Light Emitting Devices*; Wiley-VCH: Weinheim, Germany, 2005.
85. Casas, J.M.; Falvello, L.R.; Fornìe, J.; Martin, A.; Welch, A.J. Pentafluorophenyl complexes of platinum containing intramolecular Pt–H hydrogen bridging interactions. Crystal structures of [NBu₄][Pt(C₆F₅)₃ (8-hydroxyquinoline)] and [NBu₄][Pt(C₆F₅)₃ (8-methylquinoline)]. *Inorg. Chem.* **1996**, *35*, 6009–6014. [[CrossRef](#)]

86. Chen, C.H.; Shi, J. Metal chelates as emitting materials for organic electroluminescence. *Coord. Chem. Rev.* **1998**, *171*, 161. [[CrossRef](#)]
87. Wang, S. Luminescence and electroluminescence of Al(III), B(III), Be(II) and Zn(II) complexes with nitrogen donors. *Coord. Chem. Rev.* **2001**, *79*, 215. [[CrossRef](#)]
88. Li, D.; Wang, K.; Huang, S.; Qu, S.; Liu, X.; Zhu, Q.; Zhang, H.; Wang, J.Y. Brightly fluorescent red organic solids bearing boron-bridged π -conjugated skeletons. *Mater. Chem.* **2011**, *21*, 15298–15304. [[CrossRef](#)]
89. Kim, Y.; Bouffard, J.; Kooi, S.E.; Swager, T.M. Highly Emissive Conjugated Polymer Excimers. *J. Am. Chem. Soc.* **2005**, *127*, 13726. [[CrossRef](#)]
90. Wakamiya, A.; Mori, K.; Yamaguchi, S. 3-Boryl-2,2'-bithiophene as a Versatile Core Skeleton for Full-Color Highly Emissive Organic Solids. *Angew. Chem. Int. Ed.* **2007**, *46*, 4273. [[CrossRef](#)] [[PubMed](#)]
91. Ye, S.; Chen, J.; Di, C.; Liu, Y.; Lu, K.; Wu, W.; Du, C.; Liu, Y.; Shuai, Z.; Yu, G. Phenyl-substituted fluorene-dimer cored anthracene derivatives: Highly fluorescent and stable materials for high performance organic blue- and white-light-emitting diodes. *J. Mater. Chem.* **2010**, *20*, 3186–3194. [[CrossRef](#)]
92. Yao, Y.-S.; Zhou, Q.-Z.; Wang, X.-S.; Wang, Y.; Zhang, B.-W. Fine tuning of the photophysical and electroluminescent properties of DCM-type dyes by changing the structure of the electron-donating group. *J. Mater. Chem.* **2006**, *16*, 3512. [[CrossRef](#)]
93. Odom, S.A.; Parkin, S.R.; Anthony, J.E. Tetracene Derivatives as Potential Red Emitters for Organic LEDs. *Org. Lett.* **2003**, *5*, 4245–4248. [[CrossRef](#)]
94. Li, D.; Zhang, H.; Wang, C.; Huang, S.; Guo, J.; Wang, Y. Construction of full-color-tunable and strongly emissive materials by functionalizing a boron-chelate four-ring-fused π -conjugated core. *J. Mater. Chem.* **2012**, *22*, 4319–4328. [[CrossRef](#)]
95. Satrijo, A.; Kooi, S.E.; Swager, T.M. Enhanced luminescence from emissive defects in aggregated conjugated polymers. *Macromolecules.* **2007**, *40*, 8833–8841. [[CrossRef](#)]
96. Vidyasagar, C.C.; Muñoz Flores, B.M.; Jiménez-Pérez, V.M.; Gurubasavaraj, P.M. Recent advances in boron-based schiff base derivatives for organic light-emitting diodes. *Mater. Today Chem.* **2018**, *11*, 133–155. [[CrossRef](#)]
97. Wu, Z.; Wang, Q.; Yu, L.; Chen, J.; Qiao, X.; Ahamad, T.; Alshehri, S.M.; Yang, C.; Ma, D. Managing excitons and charges for high-performance fluorescent white organic light-emitting diode. *ACS Appl. Mater. Interfaces* **2016**, *8*, 28780–28788. [[CrossRef](#)] [[PubMed](#)]
98. Jung, B.J.; Yoon, C.-B.; Shim, H.-K.; Do, L.-M.; Zyung, T. Pure-Red Dye for Organic Electroluminescent Devices: Bis-Condensed DCM Derivatives. *Adv. Funct. Mater.* **2001**, *11*, 430. [[CrossRef](#)]
99. Massue, J.; Denis, F.; Ulrich, G.; Retailliau, P.; Ziessel, R. Synthesis of Luminescent 2-(2'-Hydroxyphenyl)benzoxazole (HBO) Borate Complexes. *Org. Lett.* **2012**, *14*, 230–233. [[CrossRef](#)] [[PubMed](#)]
100. Li, D.; Yuan, Y.; Bi, H.; Yao, D.; Zhao, X.; Tian, W.; Wang, Y.; Zhang, H. Boron-Bridged π -Conjugated Ladders as Efficient Electron-Transporting Emitters. *Inorg. Chem.* **2011**, *50*, 4825–4831. [[CrossRef](#)]
101. Cheng, F.; Jäkle, F. RAFT polymerization of luminescent boron quinolate monomers. *Chem. Commun.* **2010**, *46*, 3717–3719. [[CrossRef](#)]
102. Matsumi, N.; Chujo, Y. π -Conjugated Organoboron Polymers via the Vacant *p*-Orbital of the Boron Atom. *Polym. J.* **2008**, *40*, 77–89. [[CrossRef](#)]
103. Elbing, M.; Bazan, G.C. A New Design Strategy for Organic Optoelectronic Materials by Lateral Boryl Substitution. *Angew. Chem. Int. Ed.* **2008**, *47*, 834–838. [[CrossRef](#)]
104. Jäkle, F. Lewis acidic organoboron polymers. *Coord. Chem. Rev.* **2006**, *250*, 1107–1121. [[CrossRef](#)]
105. Lamère, J.F.; Lacroix, P.G.; Farfa, N.; Rivera, J.M.; Santillan, R.; Nakatani, K. Synthesis, characterization and nonlinear optical (NLO) properties of a push-pull bisboronate chromophore with a potential electric field induced NLO switch. *J. Mater. Chem.* **2006**, *16*, 2913–2920. [[CrossRef](#)]
106. Maldonado, J.L.; Ramos-Ortiz, G.; Barbosa-García, O.; Meneses-Nava, M.A.; Arquez, L.M.; Olmos-LOpez, M. Dynamic holographic imaging using photorefractive polymers based on a boronate-derivative nonlinear chromophore. *Int. J. Mod. Phys.* **2007**, *15*, 2625–2634. [[CrossRef](#)]
107. Shi, W.-J.; Lo, P.-C.; Singh, A.; Ledoux-Rak, I.; Ng, D.K.P. Synthesis and second-order nonlinear optical properties of push-pull BODIPY derivatives. *Tetrahedron* **2012**, *68*, 8712–8718. [[CrossRef](#)]
108. Reyes, H.; Muñoz, B.M.; Farfán, N.; Santillan, R.; Rojas-Lima, S.; Lacroix, P.G.; Nakatani, K. Synthesis, crystal structures, and quadratic nonlinear optical properties in a series of push-pull boronate derivatives. *J. Mater. Chem.* **2002**, *12*, 2898–2903. [[CrossRef](#)]
109. Prasad, P.N.; Williams, D.J. (Eds.) *Introduction to Nonlinear Optical Effects in Molecules and Polymers*; Wiley: New York, NY, USA, 1991.
110. Kuhn, H.; Robillard, J. (Eds.) *Nonlinear Optical Materials*; CRC Press: Boca Raton, MIA, USA, 1992.
111. Nalwa, H.S.; Miyata, S. (Eds.) *Nonlinear Optics of Organic Molecules and Polymers*; CRS Press: New York, NY, USA, 1997.
112. Verbiest, T.; Houbrechts, S.; Kauranen, M.; Clays, K.; Persoons, A. Second-order nonlinear optical materials: Recent advances in chromophore design. *J. Mater. Chem.* **1997**, *7*, 2175–2189. [[CrossRef](#)]
113. Dalton, L.R.; Harper, A.W.; Ghosn, R.; Steier, W.H.; Ziari, M.; Fetterman, H.; Shi, Y.; Mustacich, R.V.; Jen, A.K.-Y.; Shea, K.J. Synthesis and Processing of Improved Organic Second-Order Nonlinear Optical Materials for Applications in Photonics. *Chem. Mater.* **1995**, *7*, 1060. [[CrossRef](#)]

114. Reyes, H.; Rivera, J.M.; Farfán, N.; Santillan, R.; Lacroix, P.G.; Lepetit, C.; Nakatani, K. Synthesis and quadratic molecular hyperpolarizabilities of two new chiral boronates: Computational and experimental study. *J. Organomet. Chem.* **2005**, *690*, 3737–3745. [[CrossRef](#)]
115. Hawthorne, M.F.; Lee, M.W. A Critical Assessment of Boron Target Compounds for Boron Neutron Capture Therapy. *J. Neurooncol.* **2003**, *62*, 33. [[CrossRef](#)]
116. Suginome, M.; Uehlin, L.; Yamamoto, A.; Murakami, M. A New Look at Boron Enolate Chemistry: Aminative C–C Bond Formation Using Diaminoboron Enolate with Aldehyde. *Org. Lett.* **2004**, *6*, 1167. [[CrossRef](#)]
117. Kennedy, J.W.J.; Hall, D.G. Recent Advances in the Activation of Boron and Silicon Reagents for Stereocontrolled Allylation Reactions. *Angew. Chem. Int. Ed.* **2003**, *42*, 4732. [[CrossRef](#)]
118. Liu, Z.; Fang, Q.; Cao, D.; Wang, D.; Xu, G. Triaryl Boron-Based A- π -A vs Triaryl Nitrogen-Based D- π -D Quadrupolar Compounds for Single- and Two-Photon Excited Fluorescence. *Org. Lett.* **2004**, *6*, 2933. [[CrossRef](#)]
119. Entwistle, C.D.; Marder, T.B. Boron Chemistry Lights the Way: Optical Properties of Molecular and Polymeric Systems. *Angew. Chem. Int. Ed.* **2002**, *41*, 2927. [[CrossRef](#)]
120. Candeias, N.R.; Montalbano, F.; Cal, P.M.S.D.; Gois, P.M. Boronic acid and esters in the petasis-boron manich multicomponent reaction. *Chem. Rev.* **2010**, *10*, 6169–6193. [[CrossRef](#)] [[PubMed](#)]
121. Sakuda, E.; Ando, Y.; Ito, A.; Kitamura, N. Extremely Large Dipole Moment in the Excited Singlet State of Tris[*p*-(N,N-dimethylamino)phenylethynyl]duryl]borane. *J. Phys. Chem. A* **2010**, *114*, 9144–9150. [[CrossRef](#)] [[PubMed](#)]
122. Miller, D.S.; Leffler, J.E. Absorption spectra of triarylborons. *J. Phys. Chem.* **1970**, *74*, 2571. [[CrossRef](#)]
123. Matsumi, N.; Naka, K.; Chujo, Y.J. Poly(*p*-phenylene-borane)s. Novel Organoboron π -Conjugated Polymers via Grignard Reagent. *J. Am. Chem. Soc.* **1998**, *120*, 10776. [[CrossRef](#)]
124. Matsumi, N.; Kotera, K.; Chujo, Y. Alternating Boration Copolymerization between Diynes and Diisocyanates. Organoboron Polymers Bearing Monomeric Iminoborane in Their Main Chain. *Macromolecules* **2000**, *33*, 2801–2806. [[CrossRef](#)]
125. Matsumi, N.; Umeyama, T.; Chujo, Y. π -Conjugated poly(cyclodiborazane)s with intramolecular charge transferred structure. *Macromolecules* **2000**, *33*, 3956–3957. [[CrossRef](#)]
126. Matsumi, N.; Chujo, Y. Synthesis of π -Conjugated Poly(cyclodiborazane)s by Organometallic Polycondensation. *Macromolecules* **2000**, *33*, 8146–8148. [[CrossRef](#)]
127. Jia, W.-L.; Song, D.; Wang, S. Blue Luminescent Three-Coordinate Organoboron Compounds with a 2,2'-Dipyridylamino Functional Group. *J. Org. Chem.* **2003**, *68*, 701. [[CrossRef](#)]
128. Qin, Y.; Kiburu, I.; Shah, S.; Jäkle, F. Synthesis and Characterization of Organoboron Quinolate Polymers with Tunable Luminescence Properties. *Macromolecules* **2006**, *39*, 9041–9048. [[CrossRef](#)]
129. Nagata, Y.; Chujo, Y. Synthesis of Methyl-Substituted Main-Chain-Type Organoboron Quinolate Polymers and Their Emission Color Tuning. *Macromolecules* **2008**, *41*, 2809–2813. [[CrossRef](#)]
130. Nagata, Y.; Chujo, Y. Main-Chain-Type *N,N'*-Chelate Organoboron Aminoquinolate Polymers: Synthesis, Luminescence, and Energy Transfer Behavior. *Macromolecules* **2008**, *41*, 3488–3492. [[CrossRef](#)]
131. Reitzenstein, D.; Lambert, C. Localized versus Backbone Fluorescence in *N-p*-(Diarylboryl)phenyl-Substituted 2,7- and 3,6-Linked Polycarbazoles. *Macromolecules* **2009**, *42*, 773–782. [[CrossRef](#)]
132. Hudson, Z.M.; Wang, S. Impact of Donor–Acceptor Geometry and Metal Chelation on Photophysical Properties and Applications of Triarylboranes. *Acc. Chem. Res.* **2009**, *42*, 1584–1596. [[CrossRef](#)]
133. Li, H.; Jäkle, F. Facile Route to Organoboron Quinolate Polymers through Boron-Induced Ether Cleavage. *Macromolecules* **2009**, *42*, 3448–3452. [[CrossRef](#)]
134. Lorbach, A.; Bolte, M.; Li, H.; Lerner, H.-W.; Holthausen, M.C.; Jäkle, F.; Wargner, M. 9,10-Dihydro-9,10-diboraanthracene: Supramolecular Structure and Use as a Building Block for Luminescent Conjugated Polymers. *Angew. Chem. Int. Ed.* **2009**, *48*, 4584. [[CrossRef](#)]
135. Lam, S.-T.; Zhu, N.; Yam, V.W.-W. Synthesis and Characterization of Luminescent Rhenium(I) Tricarbonyl Diimine Complexes with a Triarylboron Moiety and the Study of Their Fluoride Ion-Binding Properties. *Inorg. Chem.* **2009**, *48*, 9664. [[CrossRef](#)]